Distribution Agreement

In presenting this thesis as a partial fulfillment of the requirements for a degree from Emory University, I hereby grant to Emory University and its agents the non-exclusive license to archive, make accessible, and display my thesis in whole or in part in all forms of media, now or hereafter now, including display on the World Wide Web. I understand that I may select some access restrictions as part of the online submission of this thesis. I retain all ownership rights to the copyright of the thesis. I also retain the right to use in future works (such as articles or books) all or part of this thesis.

Brittney Haney March 21, 2022

Synthetic Investigations into Small Molecules with Antibacterial Potential

by

Brittney Haney

William Wuest, Ph.D.

Adviser

Emory University Department of Chemistry

William M. Wuest, Ph.D

Adviser

Richard A. Himes, Ph.D.

Committee Member

Connie B. Roth, Ph.D.

Committee Member

2022

Synthetic Investigations into Small Molecules with Antibacterial Potential

By

Brittney Haney

William M. Wuest, Ph.D.

Adviser

An abstract of

a thesis submitted to the Faculty of Emory College of Arts and Sciences

of Emory University in partial fulfillment

of the requirements of the degree of

Bachelor of Science with Honors

Emory Department of Chemistry

2022

Abstract

Synthetic Investigations into Small Molecules with Antibacterial Potential

By Brittney Haney

Due to the rise of resistant bacteria and persister cell populations, a new demand for novel antibiotics has arisen to combat these strains before they lead to a severe infection or even death. In recognizing this issue, our work focuses on two different mechanisms of action to kill resistant and persistent bacteria. The first is membrane perturbation in which the bacterial membrane is perturbed, ultimately leading to cell death. The second mechanism is that of metallophores, such as siderophores or chalkophores, which can utilize metallophore uptake machinery to trick the bacterial cell for uptake and in turn, provide an opportunity to lead to the cells' ultimate destruction. From these mechanisms, two small molecules were identified and synthesized to analyze their potential as antimicrobial agents. The first being CD437, a synthetic retinoid that previously displayed activity through membrane perturbation. The other being SF2768 which showed promise as a bacterial chalkophore. This work will further elucidate the potential of these molecules and outline the synthetic methods used to achieve them.

Synthetic Investigations into Small Molecules with Antibacterial Potential

By

Brittney Haney

William Wuest, Ph.D.

Adviser

A thesis submitted to the Faculty of Emory College of Arts and Sciences

of Emory University in partial fulfillment

of the requirements of the degree of

Bachelor of Science with Honors

Emory University Department of Chemistry

2022

Acknowledgments

I would first like to Cassie Schrank, who taught me how to overcome the failure that frequently comes with total synthesis and chemistry in general. I have known you for three years now, and every day in the lab I grow to appreciate you more. Not only are you a great mentor, and an amazing friend, but one of the best people I have met during my time at Emory.

I would also like to thank Bill Wuest for the guidance and mentorship he has given me for over three years. You have provided me with so many opportunities, which in turn shaped my plans for the future and fostered my passion for chemistry, and for that, I can not thank you enough.

I would also like to thank my other committee members, Dr. Roth and Dr. Himes for both being an inspiration to me inside and outside of the classroom. I greatly appreciate your guidance and participation on my committee.

Table of Contents

Chapter 1- Introduction to Resistant Bacteria, Persistent Mechanisms, and Antimicrobial Compounds

It has been increasingly relevant in the past 20 years that there is a rising need for therapeutic, pathogen-specific compounds. Over time, bacteria have developed mechanisms that allow them to circumnavigate the intended effects of antibiotics. These mechanisms allow bacteria to cause more severe infections which are predicted to lead to millions of deaths worldwide by 2050.[1] The CDC has also recently reported that in the United States alone, over 2.8 million antibiotic-resistant infections occur annually, and due to these infections over 35,000 million die, making it a large public health issue.[2] Because of this substantial impact on so many people, it is crucial to identify and develop new compounds with the ability to target and eradicate these resistant bacteria often referred to as superbugs.

Single and multidrug-resistant (MDR) strains of already dangerous pathogens can develop through genetic mutations. These mutations can provide bacterial adaptations such as the ability to efflux antibiotics from the cell, modify pathways targeted by the antimicrobial agents, alter the permeability of the cell wall, and many other systematic alterations.[3] This makes these MDR strains more difficult to kill with antimicrobial agents and can lead to more severe bacterial infections. These mechanisms of resistance can also be spread through horizontal gene transfer, in which resistant genes are interchanged between organisms. When these genes are transferred, more bacteria develop that have mechanisms allowing them to dodge the immediate consequences of antibiotics, thereby further developing species that can

survive antibiotics. These resistant strains are then perpetuated through natural selection which selectively favors these mutations due to the pressure of antibiotics.

Unfortunately, resistance is not the only factor allowing bacteria to evade antimicrobial compounds. While resistant cells can continue growth in the presence of antibiotics, there is another method employed by bacteria that utilize cells that are able to remain dormant, called persister cells. Although these types of cells were identified almost 80 years ago we have yet to develop a significant strategy to combat their effects.[4] These cells present a new challenge for antibiotics and require novel molecules that can combat cells that do not employ the same processes as living cells.

Persisters are defined as bacterial cells that are genetically similar to wild-type cells but phenotypically different, which allows them to enter a nondividing state.[4] After the pressures of antibiotics are removed from the persister cells' environment, they can become active once more. This means that these cells can cause latent infections after the initial wave of antimicrobial molecules. A need is then created for alternative molecules that can potentially interrupt persister cells alongside the antibiotics to avoid recurrent infections. In recognizing the challenges presented by resistant cells and persistent cells, our lab has identified two strategies in which to target both: membrane perturbation and metallophores.

1.1: Membrane Perturbation

In recent years, there has been much exploration into possible mechanisms that are effective against persister cells. One of the most understudied mechanisms to target both persistent and resistant cells is through membrane perturbation. The membrane is essential to maintaining the integrity of any bacterial cell, as it sustains the concentrations of nutrients necessary for biological processes and physically houses the bacteria's internal components.[5] Targeting the membrane is often overlooked as a mechanism of action due to low membrane selectivity, meaning that there is potential for lysing human cells as well.[6] In recent years a slew of small molecules with the ability to target the membrane have been identified, including the synthetic retinoid CD437. Due to the dormancy of persister cells, they do not participate in the growth processes that are often exploited by antibiotics.[5] For this reason, physically lysing the gram-positive and even harder to kill gram-negative persister cells through membrane perturbation is one of the most promising ways to destroy these subpopulations of cells. This would inhibit them from returning to a dividing growth state after the pressure from antibiotics is removed.

There are two main routes in which small molecules can be used to target the bacterial membrane.[5] Inducing small holes through permeabilization of the cell membrane can lead to spillage of cellular contents or allow other molecules into the cell, which can both lead to the bacterias' destruction. Another possible mechanism is membrane depolarization where the membrane's electronic gradient is disrupted which inhibits ATP synthesis by affecting the proton motive force of the bacterial cell. This can then lead to the death of the cell or allow other

molecules to successfully disrupt and kill the cell. Both of these mechanisms can effectively target persister cells, but there are significant challenges when it comes to finding small molecules with this ability.

1.2: Metallophores

Another potential mechanism to defeat these resistant and persistent bacteria that has been identified is through the exploitation of metallophores. Specifically, our lab has focused on the potential of chalkophores and siderophores. Chalkophores are molecules that bind copper and bring the metal ions within the bacterial cell and siderophores are compounds that do the same for iron. The concentration of metal ions is key to maintaining homeostasis within a bacterial cell, and chalkophores allow this concentration to be sustained. The transition metal ions imported via metallophores are required for electron transport due to their redox capabilities and they also play a key catalytic role in many essential bacterial enzymes.[7]

It has come to our attention that these molecules can also be used as a type of trojan horse that can easily enter bacteria cells and in turn provide an opportunity to lead to the cells' ultimate destruction. The mechanism to which these metallophores exactly operate remains uncertain, but it is widely known that excess copper can damage bacterial cells through the formation of reactive oxygen species.[8] There have been several examples of chalkophores and siderophores that possess antimicrobial abilities against gram-positive bacteria. For example, the copper-binding peptide methanobactin from *Methylosinus trichosporium* OB3b has shown well documented antibacterial efficacy against gram-positive *Listeria monocytogenes* Scott A.[9] A

new bacterial chalkophore, called SF2768 with vague antibacterial qualities has come to our attention. Due to these characteristics, SF2768 became a molecule of great interest for our laboratory and we proposed a deep dive into its capabilities and mechanism of action to determine whether it could be utilized in the fight against persisters and resistant bacteria.

Chapter 2- CD437

2.1- Introduction to CD437

As mentioned in Chapter 1, membrane perturbation might be the key to eradicating persister cell populations. CD437(**1**) is a synthetic retinoid and analog of vitamin A that was found to have activity against methicillin-resistant *Staphylococcus aureus* (MRSA) (Fig 1). This molecule was discovered in an automated high-throughput *Caenorhabditis Elegans*–MRSA killing assay developed by the Eleftherios Mylonakis lab at Brown University in which they screened almost 82,000 small molecules.[10] CD437 was singled out due to its high killing rates and low probability of resistance selection. Upon its discovery, full biological analysis showed that CD437 had a low minimum inhibitory concentration (MIC) of 1 μg/mL in an *in vitro* bactericidal activity study against MRSA strain MW2. To further understand how CD437 was inducing cell death, a serial passage resistance selection assay was performed. This assay showed mutations in the genes *graS*, *yjbH,* and *manA* among the MRSA cultures it was tested on, all of which are related to membrane physiology. Consistent with these findings, CD437 was able to successfully lyse vesicles that mimicked bacterial membranes in an experiment using biomembrane-mimicking giant unilamellar vesicles. This further suggested that the mechanism of action was membrane perturbation, allowing the molecule to have activity against both wild-type and persister cells. Aiding in this hypothesis, an all-atom molecular dynamics simulation was performed and demonstrated that the carboxylic acid and the phenolic groups of the molecule attach to the surface of the membrane bilayer and from there, orthogonally implants into the membrane which then successfully perturbs the cell. Although the parent

molecule seemed promising, CD437 possesses innate toxicity toward human hepatoma cells, removing it as a viable option for therapeutic use. This then led to a collaboration with our lab to develop more potent and less toxic lead analogs.

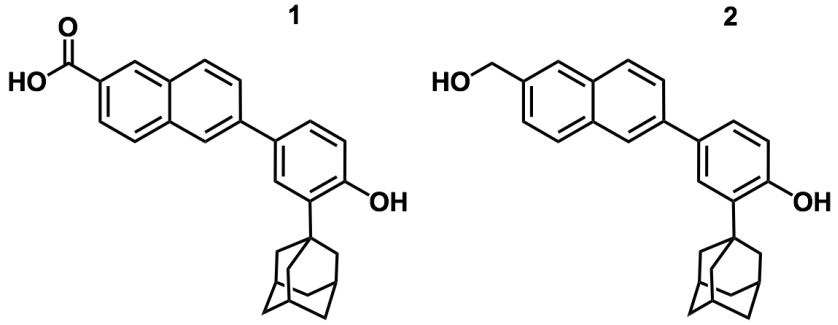

Figure 1: Structures of CD437 and Analog 2

The first generation of analog development performed by lab alums, Dr. Andrew Steele and Dr. Colleen Keohane, focused on modifications to the carboxylic acid moiety as well as the phenol moiety. Through their panel of analogs, they found a new lead analog with significant activity against both wild-type and persistent MRSA cells with an MIC of 2 μg/mL. This compound also possessed lower toxicity toward human hepatoma cells in comparison to the parent compound. This analog, denoted as Analog 2 (**2**), reduced the carboxylic group on the parent molecule with a primary alcohol. Unfortunately, this molecule possesses low solubility in serum due to significant binding to plasma binding proteins, specifically retinoid-binding proteins, meaning that it would also not work in a therapeutic setting. Since that discovery, several members of our lab including Ana Cheng and Cassandra Schrank, have synthesized two other generations of analogs.[11,12] One generation explored the adamantyl moiety of the parent scaffold, and it was found that the adamantyl was key to maintaining antibacterial capabilities.

The other generation synthesized appended an alkylamine to the hydroxyl groups of the molecule in hopes of broadening the activity of gram-negative bacteria, but unfortunately, this diminished the overall activity of the molecule.

Gathering the information collected across the previous generations, my mentor, Cassandra Schrank, and I decided to focus on our best-in-class analog, Analog 2. To eliminate the affinity of Analog 2 for the plasma binding proteins, we proposed an isosteric azaborine substitution within the molecule. This substitution would replace a carbon-carbon double bond within the naphthalene structure for a nitrogen-boron single bond which would introduce a local dipole moment into the scaffold.[13,14] Such a substitution would alter the overall electronics of the molecule by widening the HOMO-LUMO gap and hopefully alleviate the affinity issues to retinoid-binding proteins. The azaborine substitution did not have any past applications in antibiotic fields that we could find, but it was previously used in various anticancer studies dealing with T-cell lysozyme targets.[15] For these reasons, we chose to explore the impact of an azaborine substitution and determine its potential within CD437.

2.2- Synthetic Methods

To synthetically achieve the necessary substitution and synthesize the azaborine analog (**3**), we utilized the synthetic method outlined by Molander and co-workers at the University of Pennsylvania[16], in which a trifluoroborate salt (**5**) was coupled with an aminostyrene (**4, Scheme 1**). This method was chosen due to its amenability to our previous synthesis and the accessibility towards the necessary substitution. From there, we developed a retrosynthetic

analysis and uncovered that beginning with bromophenol (**7**) and an amino-bromobenzoic acid (**6**) we could achieve the desired analog (Scheme 1).

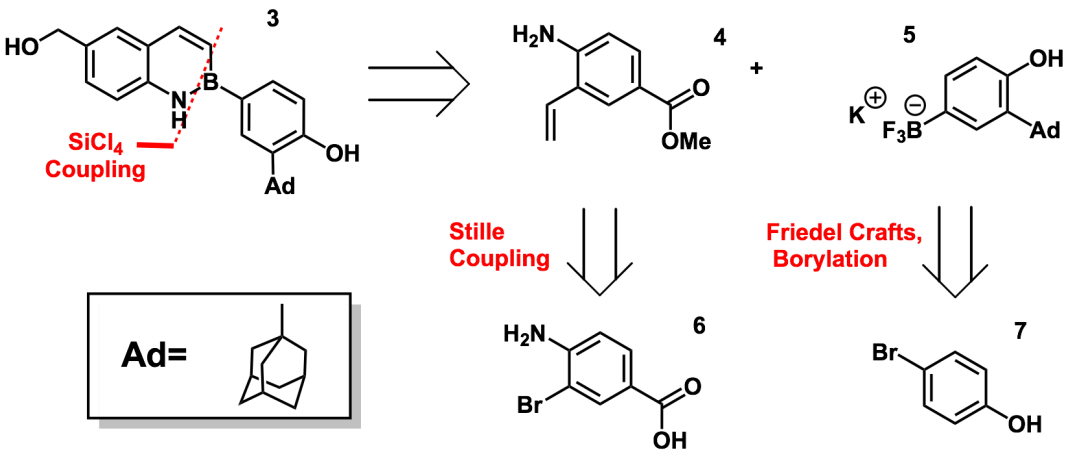

Scheme 1: Retrosynthetic Analysis for the Proposed Azaborine Analog

We then set upon synthesizing the triflouroborate salt(**5**) using the synthesis disclosed in previous works.[10,11,12,17] Beginning with the 4-bromophenol(**7**) and 1-adamantanol (**8**), we successfully achieved the borylated compound (**10**) in two steps with a 66% yield. We then used aqueous potassium bifluoride in methanol to form the necessary salt in a 62% yield.

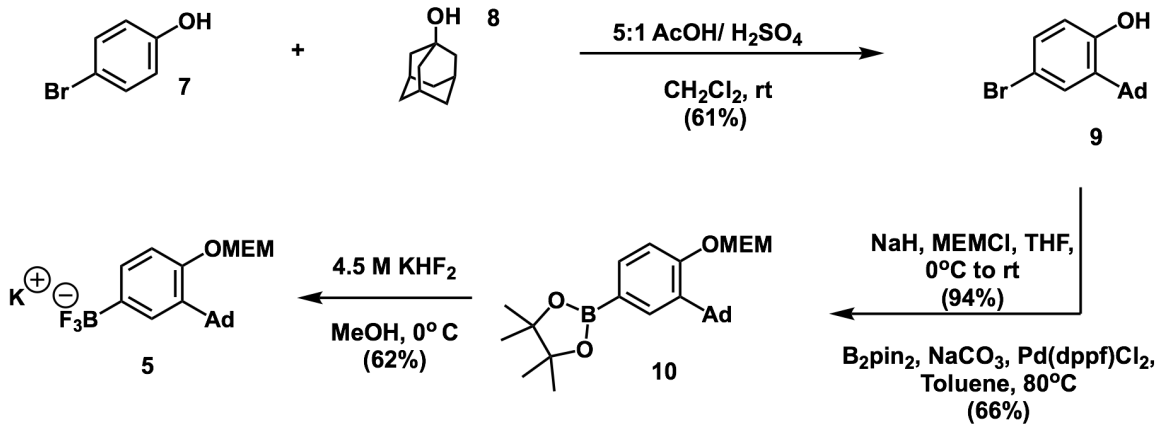

Scheme 2: Reaction Scheme for the Trifluoroborate Salt

From there, we worked to synthesize the aminostyrene fragment using a commercially available 4-amino-3-bromobenzoic acid (**6**, Scheme 3). We performed an esterification using thionyl chloride and methyl iodide and from there executed a tin-mediated vinylation to obtain the necessary aminostyrene in 80% yield.

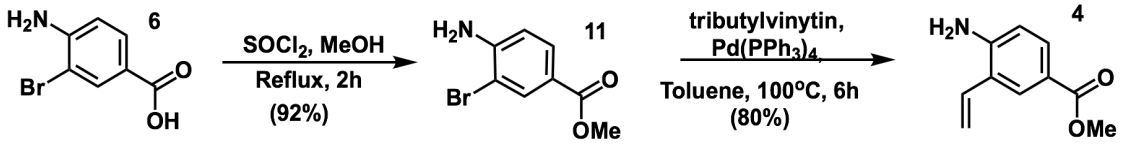

Scheme 3: Reaction Scheme for the Aminostyrene Fragment

With both fragments successfully synthesized, we performed a silicon chloride coupling to create the necessary scaffold (**12**) and achieve the azaborine substitution (Scheme 4). To then achieve our final molecule, **12** was subjected to a reduction using lithium aluminum hydride to achieve the desired analog (**3**) in 97% yield.

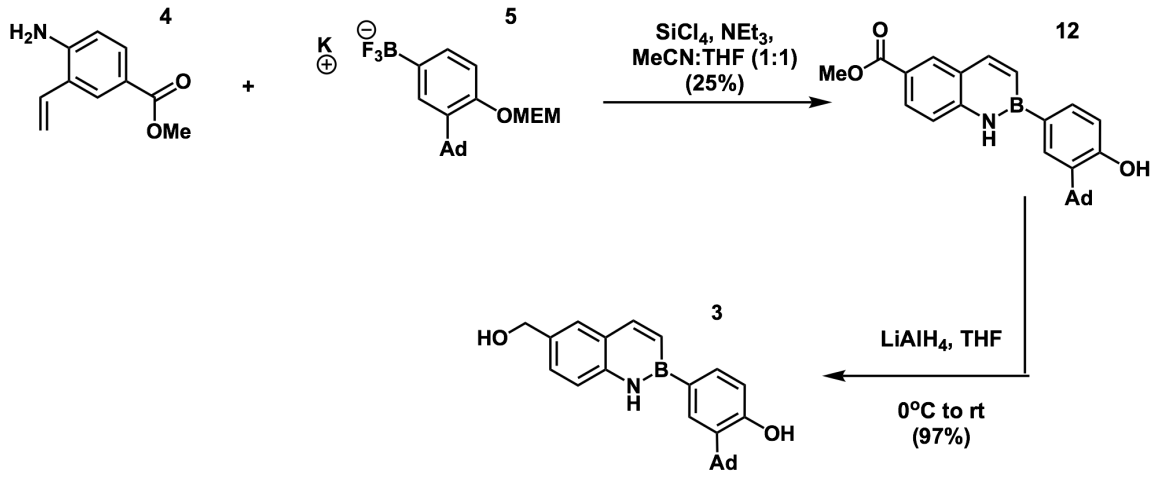

Scheme 4: Reaction Scheme to Obtain Final Azaborine analog

Originally, we attempted the same conditions outlined in the Molander synthesis[15] for the coupling, but unfortunately, this method proved difficult. Hydrochloric acid was produced during the reaction process, which removed the MEM-protecting group.[17] From there we hypothesized that deprotected free phenol then formed a new bond with the neighboring boron which would eliminate a fluoride anion that sequestered the availability of the trifluoroborate in solution for the coupling to occur. To remedy this issue triethylamine was added to the reaction in an attempt to neutralize the hydrochloric acid production, but the MEM eviction still transpired, allowing only a 25% yield for that step. In the future, a proton sponge could be used during the reaction to potentially resolve the issue.

2.3- Results and Analysis

The antibacterial capabilities of the azaborine analog were then tested in a panel against *Staphylococcus aureus* (SH1000, ATCC 33591, USA 300-0114), *Pseudomonas aeruginosa* (PAO1), *Enterococcus faecalis* (OG1RF), and *Escherichia coli* (MC4100).[18] Our positive control was benzalkonium chloride (BAC) as it was previously shown to kill bacteria using membrane perturbation and is commercially available. On top of the antibacterial analysis, a toxicity screening was done using a red blood cell (RBC) lysis assay and the results are documented under $Lysis_{20}$.

Compound	Minimum Inhibitory Concentration (μM)						$Lysis_{20}$ (μM)
	MSSA	HA-MRSA	CA-MRSA	*E. faecalis*	*P. aeruginosa*	*E. Coli*	
BAC	2	4	4	125	125	32	32
2	2	2	2	>250	>250	>250	125
3	125	64	250	>250	>250	>250	250

Table 1: Antimicrobial activity and toxicity data for analog 2 (**2**) and azaborine analog (**3**)

All data was obtained through an average of the highest value of three independent trials; all trials were within one dilution. Lysis assay results are measured as the concentration that lyses 20% or less of RBC.

Modified from: Haney, B.A.; Schrank, C.L.; Wuest, W.M., Synthesis and biological evaluation of an antibacterial azaborine retinoid isostere, *Tet. Let.*, 2021, **62**

To our surprise, the new analog had a higher MIC than Analog 2 for all bacterial strains, and the toxicity was comparable to the parent compound. To uncover the reason for this loss of activity, the partition coefficients for the azaborine analog and analog 2 were experimentally found using extraction protocols with *n*-octanol and deionized water.[19] These were then compared to theoretically calculated values that were found using ChemDraw-3D. Using that data, the log(base 10) of P was calculated and it was determined that Analog 2 had a logP of 0.93 while the azaborine analog had a logP of 0.12. This indicates that the isosteric substitution in **3** creates a more hydrophilic compound in comparison.

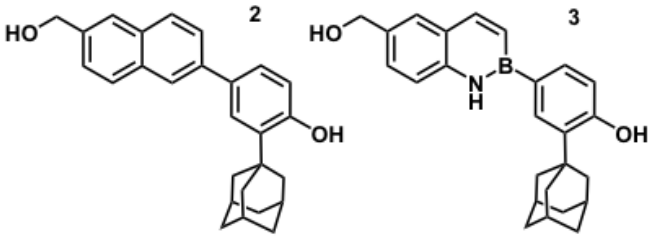

	2	3
P	9.15	1.39
logP	0.93 ± 0.20	0.12 ±0.19
cP[a]	7.687	6.792
clogP[a]	0.89	0.83
QM Dipole (D)	2.42	1.34

Table 2: Experimentally determined P and logP for analog 2 (2) and azaborine analog (3) as well as quantum mechanical calculated dipole expressed as debye (D).

Partition coefficients are shown as an average over 3 independent trials. logP data shown with + / – standard deviation. a "c" indicates calculated data for the partition coefficient utilizing the ChemDraw3D program.

Modified from: Haney, B.A.; Schrank, C.L.; Wuest, W.M., Synthesis and biological evaluation of an antibacterial azaborine retinoid isostere, *Tet. Let.*, 2021, **62**

To further elucidate these findings a quantum mechanical analysis with Schrodinger 2020-3 suite modeling software was used to find the dipole moment of each compound. From these results, it was determined that the azaborine analog had a smaller dipole moment of 1.34 D compared to 2.42 D, which was opposite of our expectations. This substitution, therefore, limits the amphiphilicity of the molecule and thus the overall ability for it to perturb the

bacterial membrane. The phenol dipole was also shown to be reduced which we believe to be due to resonance induction into the boron atom, which also disturbs the attachment to the outside of the membrane.

Chapter 3- SF2768

3.1- Introduction to SF2768

Another small molecule that showed promising antimicrobial properties was SF2768 (**13**), a diisonitrile natural product. This molecule was first isolated from *Streptomyces sp.* SF2768 and showed promise as both an antibacterial and antifungal agent.[20] From its discovery, a study was done by the Ueda lab of Nihon University showed the molecule was triggered by monesin in *S. griseorubiginosus* strain 574.[21] Since these findings, SF2768 was classified as a bacterial chalkophore and product of the putative nonribosomal peptide synthetase (NRPS) biosynthetic gene cluster within *Streptomyces thioluteus* by the He lab at Huazhong Agricultural University.[21] A biosynthetic pathway for the molecule was also proposed in this study which utilized three crucial NRPS-related enzymes.

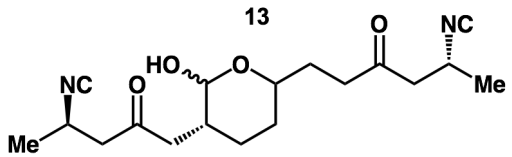

SF2768

Figure 2: Structure of SF2768

Since this discovery, a total synthesis of the molecule was performed by Yao Xu and Derek Tanto to analyze the copper-binding abilities of the molecule. It was discovered in

HR-ESI-MS-based titration experiments that SF2768 binds preferentially to Cu(I) and Cu(II), in a 2:1 stoichiometry.[20] From there, NMR titrations of linear versions of the molecule provided evidence towards a Cu-quadrupole coupling and further developed the idea that these chalkophores bind copper in a two-to-one fashion. These results also indicated that SF2768 was chelating to the metal through the two isonitrile groups on the chain of the molecule. As mentioned previously, metallophores could possess a unique mechanism against bacteria that have not been found, and they may provide easy access to the inside of bacterial cells. The characteristics of this molecule might help elucidate how this compound works as an antibiotic and warrant further analysis.

There is also extensive evidence linking isonitrile groups to antibacterial abilities. One prominent example is xanthocillin X which was isolated from *Penicillium notatum* in 1948 and was shown to have broad-spectrum antimicrobial abilities.[23] Interestingly, xanthocillin X demonstrated no notable copper-binding, and the mechanism of action was determined to be a conserved mutation in a heme biosynthesis enzyme through binding of the isonitrile. With this in mind, it could be the isonitrile moieties giving SF768 its antibacterial capabilities, which further interested our group in a developed study of several analogs of the molecule. Our group then decided to synthesize the linear versions of SF2768 as well as several analogs pictured below in order to determine more about the mechanism of action and see if these molecules which were more accessible available could be useful antimicrobial agents.

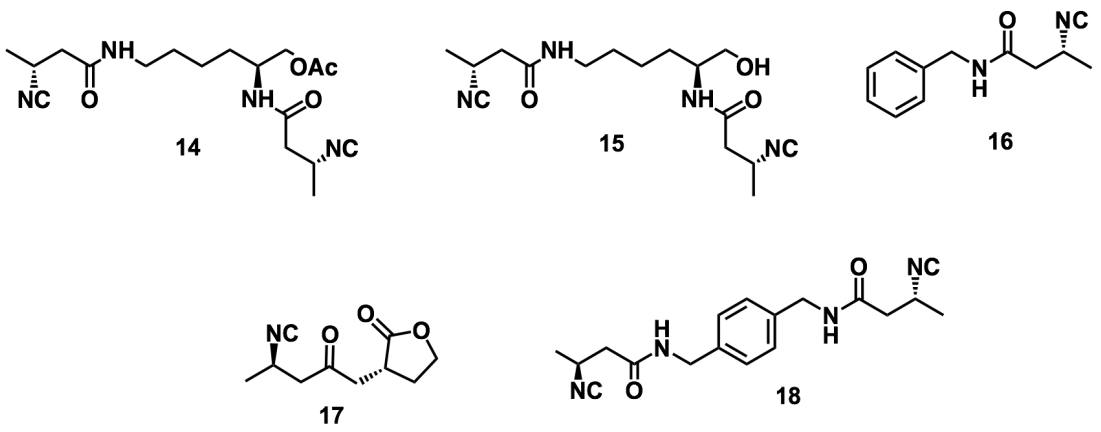

Figure 3: Structures of Linear SF2768 and other Proposed Isonitrile Analogs

3.2- Synthetic Methods

The previously mentioned total synthesis of SF2768, by Tan and coworkers[20], also provided a succinct route to the two linear analogs of SF2768 (**14,15**) so we followed the methods described in that study that couples two side-chains with a central carbon chain. To begin, the sidechains were synthesized using 3-aminobutanoic acid (**19**) that was converted into the NHS-protected isonitrile (**22**) in 3 steps in 66% yield.

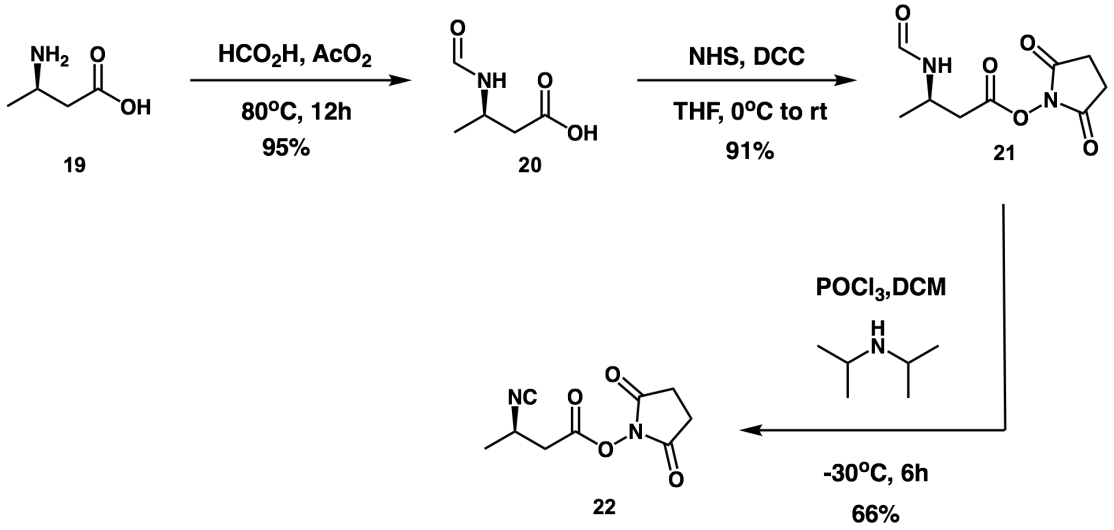

Scheme 5: Sidechain Synthetic Route

From there the main scaffold was synthesized, beginning with **23**, and in three steps, we obtained the salt (**26**) necessary for the coupling with the sidechain. After the coupling, we were able to achieve the first linear version of the molecule (**14**) in a 52% yield. From there, the acetate group on the end of the molecule was converted to an alcohol affording the second linear molecule (**15**) in 77% yield.

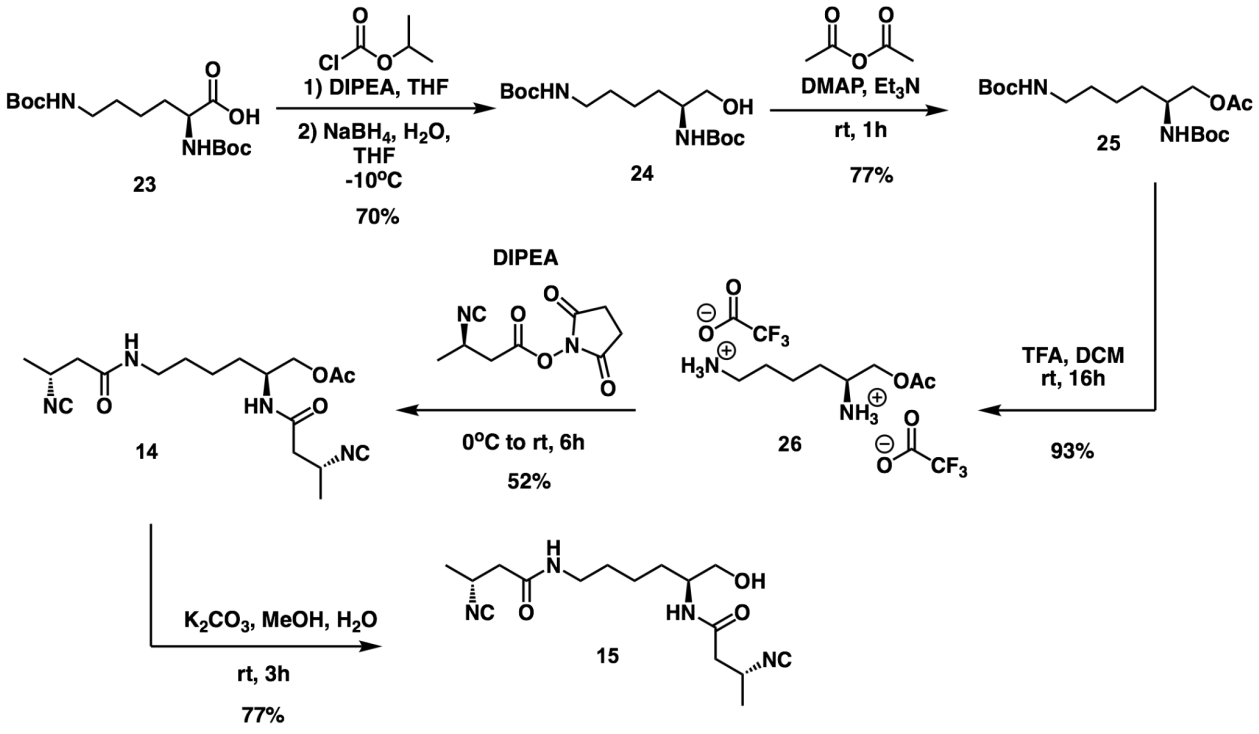

Scheme 6: Final Steps Towards the Linear Versions of SF2768

After successfully obtaining the linear versions of SF2768, I worked towards the synthesis of the benzylamine analog (**16**). Beginning with the previously synthesized sidechain molecule, a coupling was performed with phenylmethylamine and the analog was achieved in one step with a 57% yield. The other necessary analogs were completed by Cassandra Schrank.

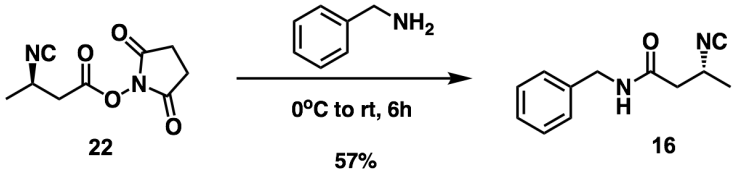

Scheme 7: Steps Towards Benzylamine Analog

3.3- Results and Analysis

With molecules in hand, we performed a growth assay against 7 different bacteria (*P. aeruginosa*, *A. baumannii*, *S. aureus*, CA-MRSA, HA-MRSA, *E. coli*, *E. faecalis*) in an attempt to determine the MIC of the molecule. To our surprise, the molecules did not have a visual MIC, despite previous findings outlining its antimicrobial activity. We wondered if this could be a result of the molecule binding to copper prematurely, so we attempted to alleviate the issue by repurifying the compounds. This strategy unfortunately did not have an effect on the growth assay results.

From there, Cassandra Schrank re-analyzed the activity of the compounds by measuring the optical density at 600 nm (OD_{600}) across all panels of bacteria with compound concentrations ranging from 500 µM to 0.119 nM. Through this analysis, it was found that our molecules had specific activity against the gram-negative pathogen, *A. baumannii,* with the two linear analogs yielding a half-maximal inhibitory concentration (IC_{50}) of 15.25 µM (acetate) and 8.856 µM (alcohol) against *A. baumannii*. Further biological studies need to be performed to further elucidate the mechanism of action of these compounds.

Chapter 4- Final Remarks

Looking at the CD437 project, we did not achieve the hypothesized results, but we were able to successfully synthesize the first azaborine analog of CD437 in 7 succinct steps. While the activity of this molecule was not substantial, we found surprising physicochemical properties that are important to document. These properties have the potential for other possible pharmaceutical applications and inspire further analysis into using this substitution with other antimicrobial natural products. Analog 2 still remains a possible antimicrobial option, but further studies are needed to determine a viable way to reduce the binding to plasma binding proteins while maintaining minimal toxicity.

The SF2768 project afforded several new analogs that were synthetically accessible in a few steps. From there, an explicit MIC could not be found but significant IC_{50} data was found which demonstrated that several of the analogs had specific activity against *A. baumannii*. This result warrants further studies into the mechanism of action for the molecule, to unearth exactly how and why the molecules are only selective for one type of bacteria. These results seem to suggest that the isonitrile groups on the molecules could potentially be interrupting a biosynthetic pathway within the bacteria, similar to xanthocillin.

Supplementary Information:

CD437

Biology

For all minimum inhibitory concentration (MIC) assays, bacteria were grown in 5 mL of Mueller-Hinton broth (tryptic-soy broth for ATCC 33591) overnight with shaking at 37˚C. Lab strains of bacteria are as follows: methicillin susceptible *Staphylococcus aureus* (SH1000), hospital-acquired methicillin resistant *Staphylococcus aureus* (ATCC 33591), community-acquired methicillin resistant *Staphylococcus aureus* (USA 300-0114), *Pseudomonas aeruginosa* (PA01), *Enterococcus faecalis* (OG1RF), and *Escherichia coli* (MC4100).

Minimum Inhibitory Concentration assays

Each compound was serially diluted from 10% DMSO in sterile DI water (v/v) stock solutions with sterile DI water to yield 12 concentrations ranging from 500 μM to 0.250 μM. The overnight cultures for each bacterium were then inoculated into 5 mL of their respective fresh media and grown until exponential phase. Once in exponential phase, each bacteria was diluted to ca. 10^6 CFU/mL in Mueller-Hinton broth and 100 μL was added to each well of 96 well U-bottom plates (VWR 15705-064) containing 100 μL of each concentration to yield test concentrations ranging from 250μM to 0.125 μM. The bacteria were grown for 22-23 hours at 37˚C before visual inspection for the MIC, which was determined as the lowest concentration at which no growth could be seen to the naked eye over three independent trials. 10% DMSO in sterile DI water served as the positive control to confirm the concentration of DMSO was not responsible for cell death. Mueller-Hinton Broth served as the negative control, showing that the media was not contaminated.

Red Blood Cell (RBC) Lysis Assay (Lysis20)

RBC lysis assay was performed on mechanically defibrillated sheep's blood (Hemostat Labs: DSB030). 1.5 mL of sheep's blood was pipetted into sterile microcentrifuge tubes and centrifuged at 10,000 rpm for ten minutes. The supernatant was removed, and the cells were resuspended in 1 mL of sterile phosphate-buffered saline (PBS) solution. This process of centrifugation, removal of supernatant, and resuspension was repeated three more times, or until the supernatant was a faint red. The final suspension was diluted 20-fold into sterile PBS buffer (30 mL) and added to serially diluted compound in 96 well U-bottom plates as described above, with test concentrations ranged from 250 μM to 0.125 μM. The cells were incubated at 37˚C with shaking for one hour, then centrifuged at 3,500 rpm for ten minutes. 100 μL of the supernatant from each well was transferred to a 96 well flat-bottom plate (Falcon 15705-066) and the absorbance was measured at 540 nm. Triton X served as the positive control (100% lysis marker) and PBS buffer served as the negative control (0% lysis marker).

Chemistry

***General Methods*:** NMR spectra were recorded using the following spectrometers: Varian INOVA400, Varian INOVA500, VNMR400, and Bruker Ascend 600. Chemical shifts are quoted in ppm relative to the indicated solvents. The following abbreviations are used to describe splitting: s (singlet), d (doublet), t (triplet), q (quartet), m (multiplet), and dd (doublet of doublets). Accurate mass spectra were recorded using a Thermo LTQ-FTMS. Non-aqueous reactions were performed using flame-dried glassware under an atmosphere of Argon with HPLC-grade solvents purified on a Pure Process Technology solvent purification system. Brine refers to a saturated solution of sodium chloride, sat. Na_2CO_3 to a saturated aqueous solution of sodium carbonate, sat. $NaHCO_3$ to a saturated solution of sodium bicarbonate, and $MgSO_4$ to magnesium sulfate. Column chromatography was performed using a Biotage® flash chromatography purification system. Chemicals were used as received from Oakwood, Sigma-Aldrich, Alfa Aesar, or AK Scientific. All final compounds were assessed for >95% purity using an Agilent Technologies 1100 Series HPLC with the following parameters: 5µm 9.4 x 250mm FLOW column, a mobile phase gradient of water-acetonitrile dosed with 0.1% formic acid, and a MWD UV/Vis Detector.

Partition Coefficient Experiments

Compound of interest was weighed for three triplicate trials into tared screwcap vials. Each was suspended into 0.5mL of 1-octanol followed by addition of 0.5mL of deionized water. The mixture was vortexed for 2 mins followed by sonication at room temperature for 5 mins. The mixture was then allowed to rest for 1 min, or until visible layers were formed. The organic layer was then extracted from the aqueous layer and placed into a separate tared vial. Both were concentrated *in vacuo*. Once dry, residual compound was measured by mass in both vials. To calculate the partition coefficient (P) the concentration of compound in both the aqueous and organic layer was first determined by calculating the amount of mmoles of compound in both followed by dividing this by 0.5mL to obtain molarity. Then the concentration of organic layer divided by the concentration of the aqueous to obtain P. This value was then subject to $\log_{10}$ to obtain logP. See sample calculations below.

$$P = \frac{[C_{octanol}]}{[C_{water}]}$$

$$\log_{10} P = \log_{10}\left(\frac{[C_{octanol}]}{[C_{water}]}\right)$$

Where C is the concentration of compound in molarity.

Schrodinger Modeling for Dipole Moment Calculations

Analogue 2 and Azaborine analog were subjected to the Ligprep protocol (default settings) as launched from within the Schrodinger 2020-3 suite of modeling software. The two compounds were then subjected to a flexible alignment to ensure that they held near-identical conformations. A structure optimization was then performed using the Jaguar Optimization panel as launched from within the Schrodinger 2020-3 suite of software. Density Functional Theory was utilized for this process with an accuracy level set to fully analytic. The maximum number of steps was set to 1000 and the PBF Water solvent model was employed. All other settings were default. At the end of the optimization, the two structures retained near-identical conformations.

[10] (3-((3r,5r,7r)-adamantan-1-yl)-4-((2-methoxyethoxy)methoxy)phenyl)trifluoroborate. Borylated compound [10] (1.0 eq, 174 mg, 0.394 mmol) was dissolved in 2.0 mL of methanol. Once dissolved, the solution was cooled to 0°C. Then an aqueous solution of potassium bifluoride (~4.5M aq, 4.0 eq, 0.40 mL) was added dropwise. The reaction was warmed slowly to room temperature. After stirring for 30 minutes, the white solid formed was filtered and washed with diethyl ether and water. After drying, a white solid was obtained (102 mg, 62% yield). **^{1}H NMR** (400 MHz, Acetone) δ 7.41 (d, J = 1.6 Hz, 1H), 7.23 (dd, J = 7.9, 1.6 Hz, 1H), 6.88 (dd, J = 8.0, 0.8 Hz, 1H), 5.24 (s, 2H), 3.83 – 3.80 (m, 2H), 3.56 – 3.53 (m, 2H), 3.30 (s, 3H), 2.80 – 2.78 (m, 2H), 2.14 (d, J = 3.0 Hz, 6H), 1.79 (s, 7H). **^{13}C NMR** (151 MHz, Acetone) δ 155.74, 136.22, 131.09, 130.57, 114.09, 94.60, 72.59, 68.67, 58.92, 42.08, 41.70, 38.15, 37.96, 37.62. **HRMS:** Accurate Mass (ES–): found 382.20549, $C_{20}H_{27}O_3BF_3$ (M–K+), requires 382.20471.

[4] Methyl 4-amino-3-vinylbenzoate. Methyl 4- amino- 3- bromobenzoate [12] (1.0 eq, 1.05g, 4.58 mmol) and tetrakis(triphenylphosphine)palladium(0) (10 mol%, 0.53g) were dissolved in 23 mL of toluene. To this mixture, tributylvinyl tin (1.13 eq, 1.51 mL, 5.17 mmol) was added in one portion. The reaction was then stirred at 100°C for ~6 h. Once complete by TLC, the reaction mixture was filtered through celite and rinsed with ethyl acetate (40 mL). The filtrate was then quenched with water (40 mL). The organic layer was extracted (3x, 20 mL) and washed with brine (20 mL). The combined organic layers were then dried with magnesium sulfate, concentrated, and purified by flash chromatography in a gradient of hexanes to ethyl acetate to afford the product as an orange solid (811 mg, 80% yield). **^{1}H NMR** (600 MHz, CDCl3) δ 7.96 (d, J = 2.0 Hz, 1H), 7.74 (dd, J = 8.4, 2.1 Hz, 1H), 6.67 (dd, J = 17.4, 11.0 Hz, 1H), 6.62 (d, J = 8.4 Hz, 1H), 5.66 (dd, J = 17.3, 1.3 Hz, 1H), 5.33 (dd, J = 11.1, 1.3 Hz, 1H), 4.27 (s, 2H), 3.84 (s, 3H). **^{13}C NMR** (151 MHz, CDCl3) δ 167.27, 148.23, 131.79, 130.48, 129.49, 122.81, 119.72, 116.87, 114.87, 51.65. **HRMS**: Accurate Mass (+pAPCI): found 178.08633, $C_{10}H_{12}O_2N$ (M+H+), requires 178.08626.

[12] Methyl 2-(3-((3r,5r,7r)-adamantan-1-yl)-4-hydroxyphenyl)-1,2-dihydrobenzo[e][1,2]azaborinine-6-carboxylate. In an oven dried microwave vial equipped with a stir bar, [**5**] (1.0 eq, 177 mg, 0.420 mmol) was charged. This vial was then evacuated and backfilled with argon 3x. In a separate vial [**6**] (1.2 eq, 89.3 mg, 0.504 mmol) was dissolved in a 1:1 mixture of acetonitrile and toluene (0.25 M, 1.67 mL). This solution was then added to the trifluoroborate salt under argon. Stirring vigorously, triethylamine (1.5 eq, 0.10 mL, 0.629 mmol) was added dropwise followed by a dropwise addition of silicon tetrachloride (2.0 eq, 0.10 mL, 0.839 mmol). The reaction was then heated to 50°C for 18 h. Upon completion, the reaction was diluted with hexanes and flushed through a silica plug which was rinsed and collected into three different fractions with dichloromethane (250 mL), a 4:1 hexanes to ethyl acetate mixture (250 mL), and finally ethyl acetate (250 mL). Each collected fraction was then concentrated and subjected to flash chromatography in a gradient of hexanes and ethyl acetate to afford a white solid (43.8 mg, 25% yield). **^{1}H NMR** (600 MHz, $CDCl_3$) δ 8.37 (s, 1H), 8.11 (d, *J* = 11.7 Hz, 2H), 8.08 (dd, *J* = 8.5, 1.9 Hz, 1H), 7.79 (d, *J* = 1.7 Hz, 1H), 7.65 (dd, *J* = 7.8, 1.6 Hz, 1H), 7.35 (d, *J* = 8.5 Hz, 1H), 7.30 (dd, *J* = 11.7, 1.9 Hz, 1H), 6.78 (d, *J* = 7.8 Hz, 1H), 5.01 (s, 1H), 3.95 (s, 3H), 2.22 (s, 6H), 2.13 (s, 3H), 1.82 (s, 6H). **^{13}C NMR** (151 MHz, $CDCl_3$) δ 167.22, 156.73, 145.44, 143.75, 136.27, 132.08, 131.96, 129.26, 125.10, 122.82, 118.30, 117.15, 52.18, 40.78, 37.24, 37.00, 29.21. **HRMS:** Accurate Mass (+pAPCI): found 413.22663, $C_{26}H_{29}O_3NB$ ($M+H^+$), requires 413.22713.

[3] 2-((3r,5r,7r)-adamantan-1-yl)-4-(6-(hydroxymethyl)benzo[e][1,2]azaborinin-2(1H)-yl)phenol.
To a flame dried round bottom flask equipped with a stir bar, lithium aluminum hydride (1.1 eq, 0.7 mg, 0.0186 mmol) was dissolved in 0.14 mL of diethyl ether (0.12 M). This mixture was then cooled to 0°C. A solution of [**13**] (1.0 eq, 7 mg, 0.0169 mmol) dissolved in 0.14 mL of diethyl ether (0.12 M) was added dropwise. The reaction mixture was then warmed to room temperature and stirred at room temperature for 2 h. Upon completion, the reaction was cooled to 0°C. Once cool, 0.14 mL of water followed by 0.14 mL of 1.0M aqueous NaOH were added. This slurry was then filtered over celite and washed with ethyl acetate (5 mL). The filtrate was then extracted with ethyl acetate (3x). Combined organic layers were washed with brine (5 mL) and water (5 mL), dried with magnesium sulfate, concentrated, and subjected to flash chromatography with a gradient of hexanes and ethyl acetate to afford a tan solid (6.3 mg, 97% yield). **^{1}H NMR** (600 MHz, $CDCl_3$) δ 8.07 (d, *J* = 11.5 Hz, 1H), 8.02 (s, 1H), 7.79 (s, 1H), 7.67 – 7.60 (m, 2H), 7.45 (dd, *J* = 8.3, 1.9 Hz, 1H), 7.33 (d, *J* = 8.3 Hz, 1H), 6.77 (d, *J* = 7.7 Hz, 1H), 5.12 (s, 1H), 4.77 (s, 2H), 3.35 (s, 2H), 2.62 (s, 5H), 2.22 (s, 5H), 2.12 (s, 3H). **^{13}C NMR** (151 MHz, $CDCl_3$) δ 156.47, 145.09, 140.12, 136.15, 133.41, 131.78, 128.20, 127.78, 125.62, 118.56, 117.07, 77.37, 77.16, 76.95, 65.49, 56.14, 41.13, 37.26, 36.98, 29.51, 29.23. **HRMS** Accurate mass (–pAPCI): found 383.21739, $C_{25}H_{27}O_2NB$ ($M–H^+$) requires 383.21766.

Spectra

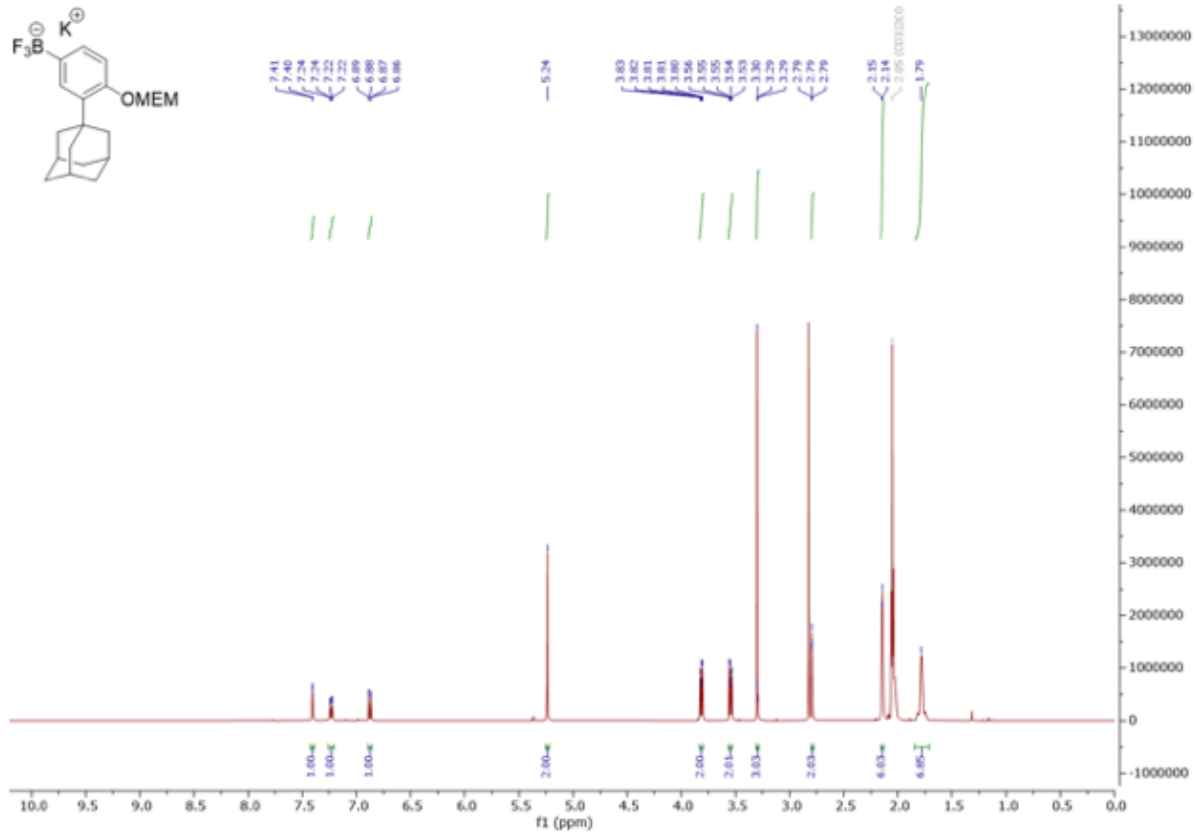

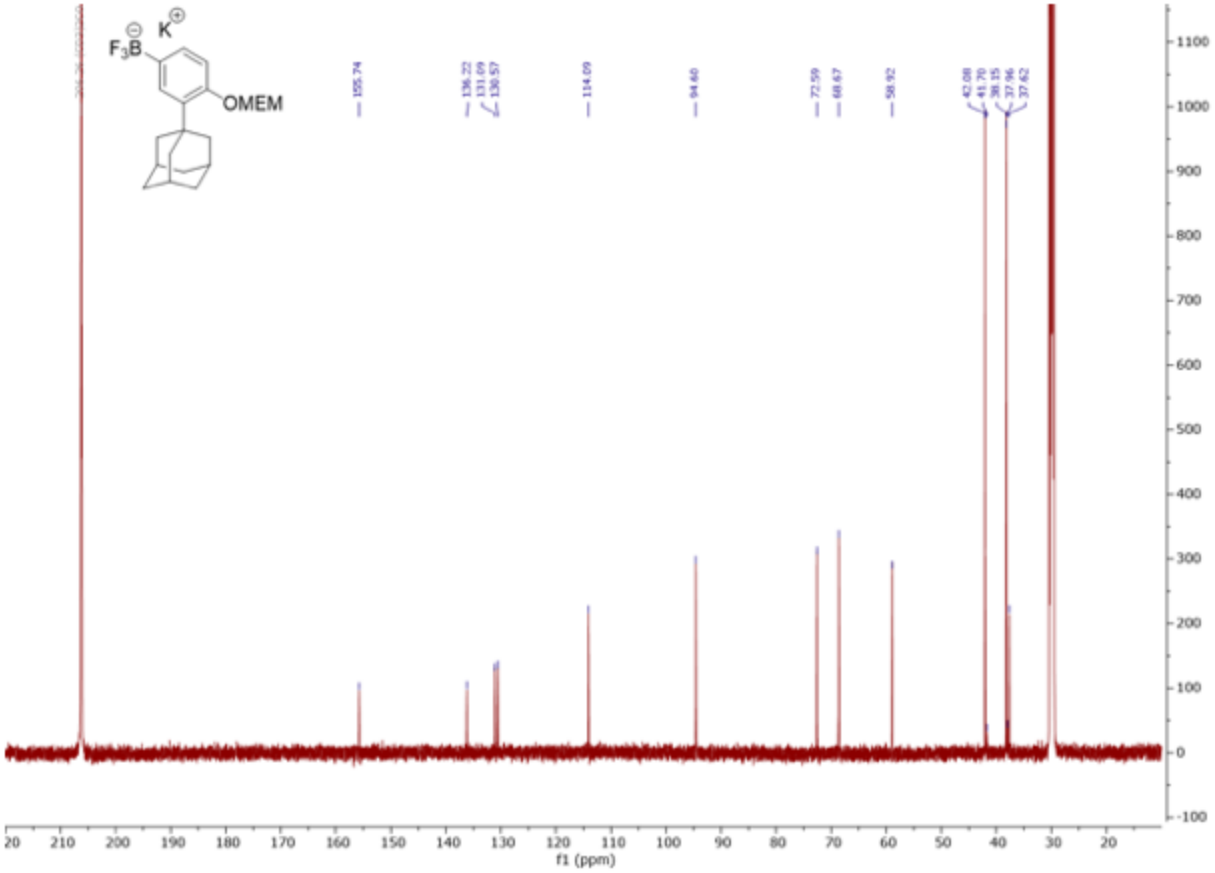
F3B
K
OMEM
155.74
136.22
133.69
130.57
114.09
94.46
72.59
68.67
58.92
42.08
41.70
38.15
37.96
37.62
f1 (ppm)

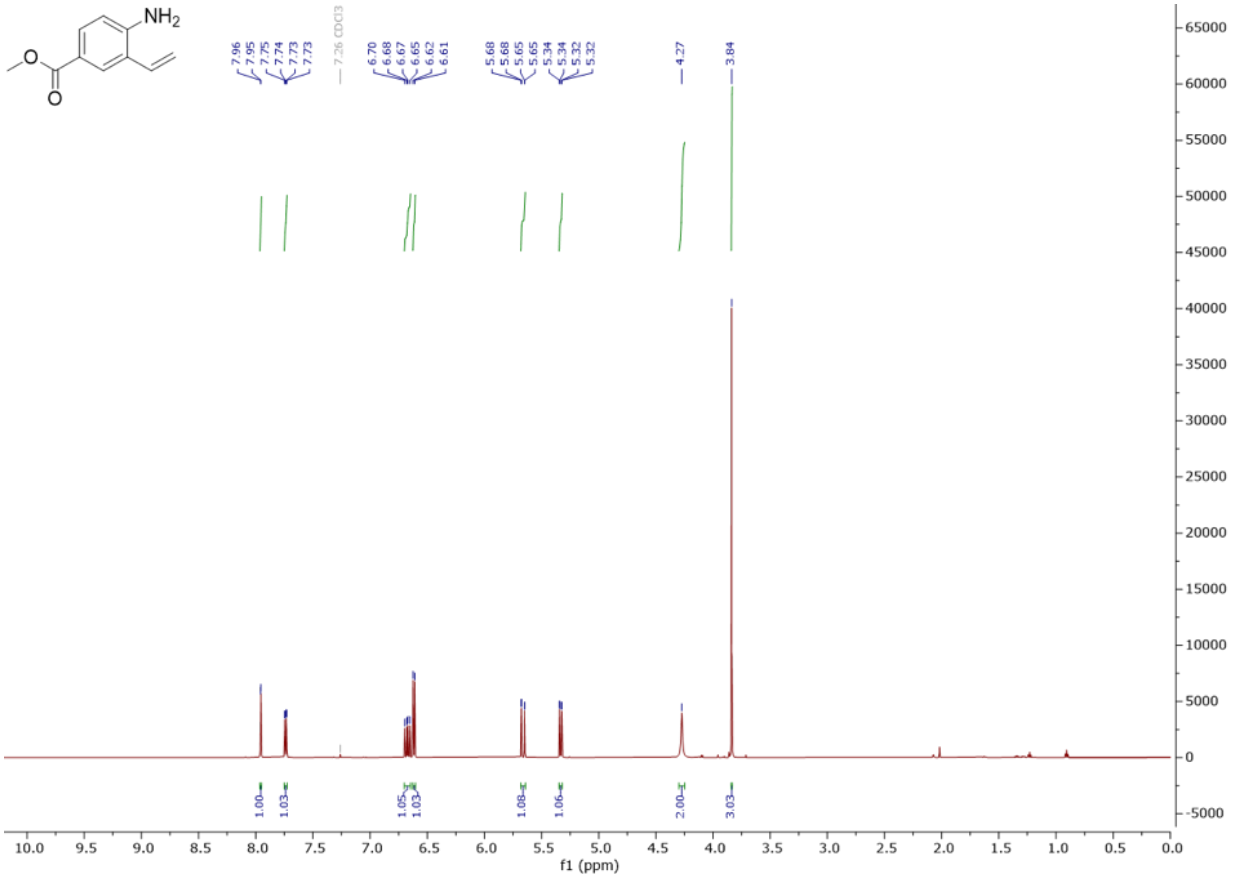
NH2
O
O
7.96
7.95
7.75
7.74
7.73
7.73
7.26 CDCl3
6.70
6.68
6.67
6.65
6.62
6.61
5.68
5.68
5.65
5.65
5.34
5.32
5.32
4.27
3.84
1.00
1.03
1.05
1.03
1.08
1.06
2.00
3.03
f1 (ppm)

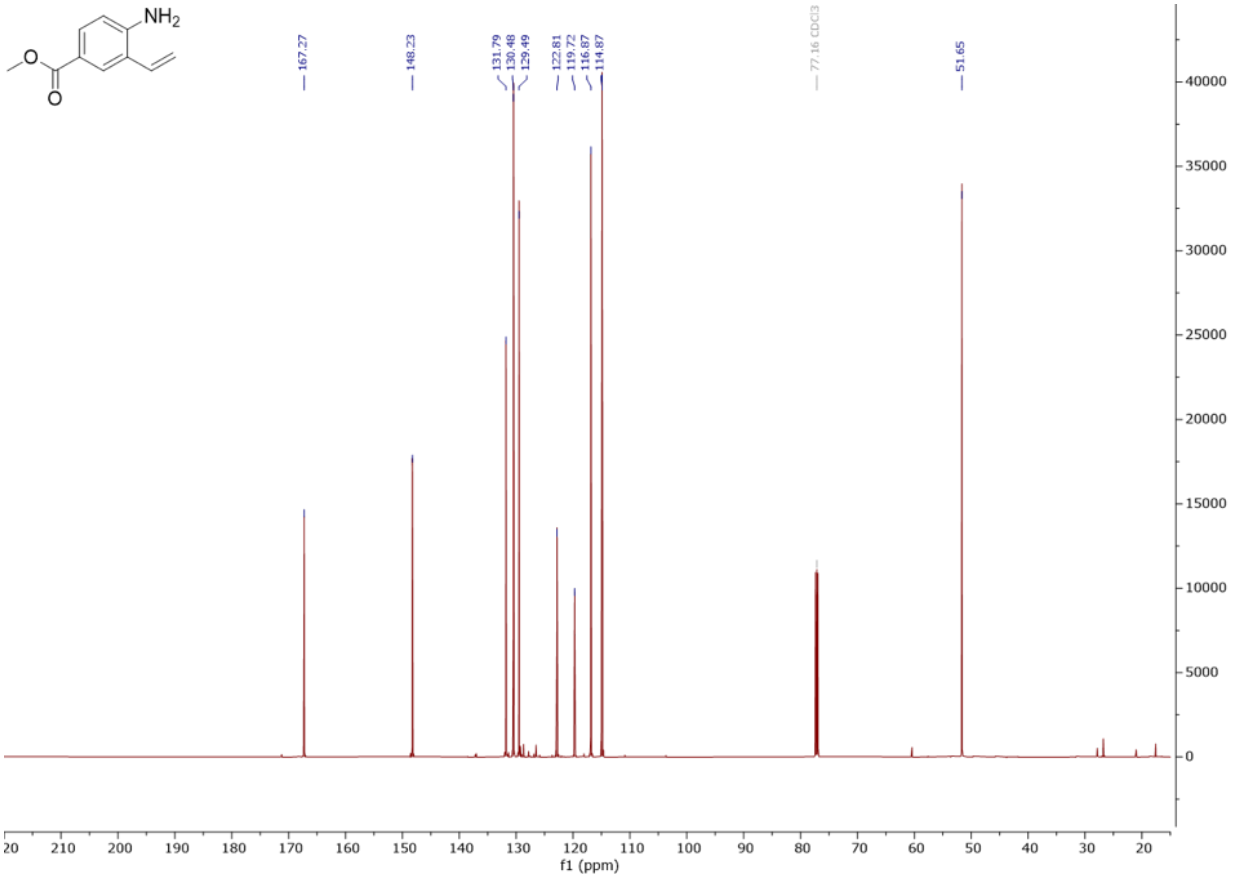
NH2
O
O
167.27
148.23
131.79
130.48
129.49
122.81
119.72
116.87
114.87
77.16 CDCl3
51.65
40000
35000
30000
25000
20000
15000
10000
5000
0
f1 (ppm)

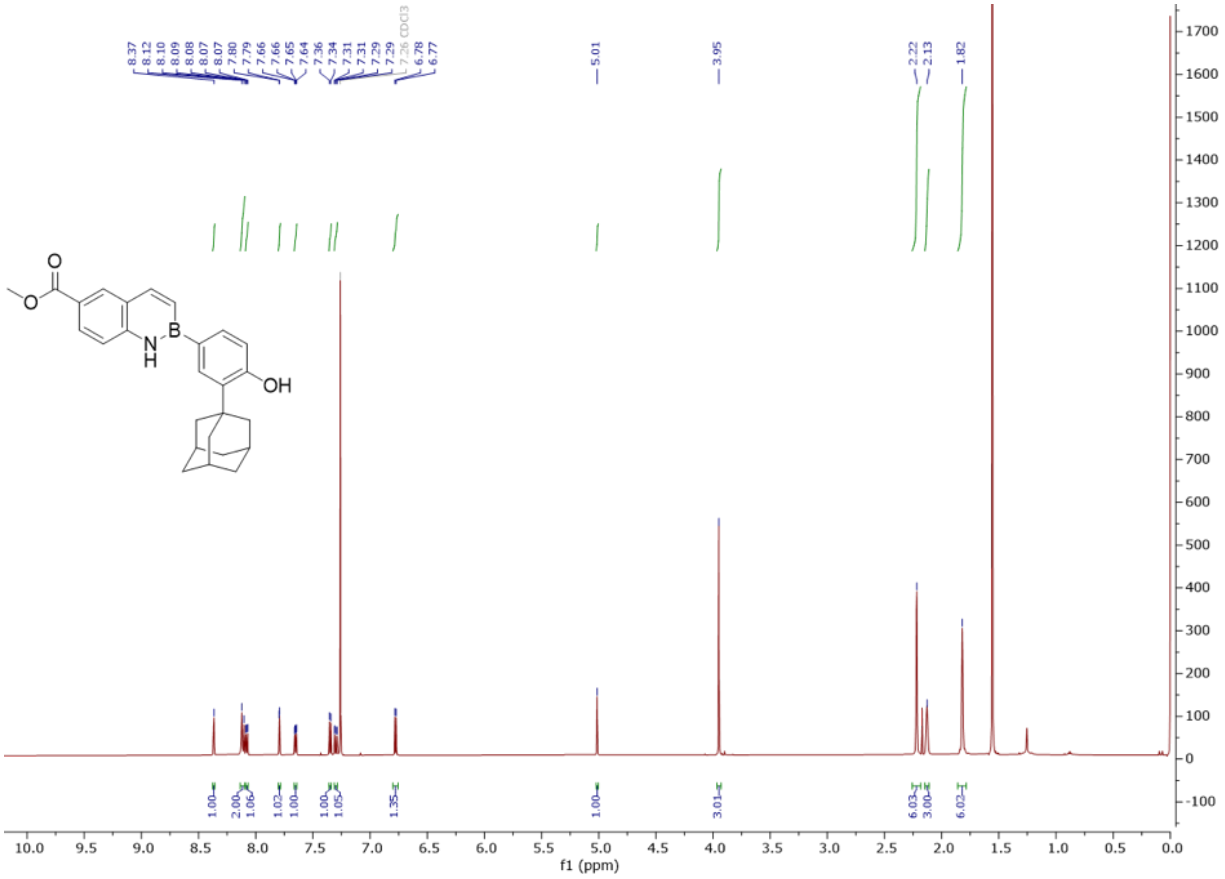
8.37
8.12
8.10
8.09
8.08
8.07
8.07
7.80
7.79
7.66
7.66
7.65
7.64
7.36
7.34
7.31
7.31
7.29
7.29
7.26 CDCl3
6.78
6.77
5.01
3.95
2.22
2.13
1.82
O
O
N
H
B
OH
1.00
2.00
1.06
1.02
1.00
1.00
1.05
1.35
1.00
3.01
6.03
3.00
6.02
f1 (ppm)

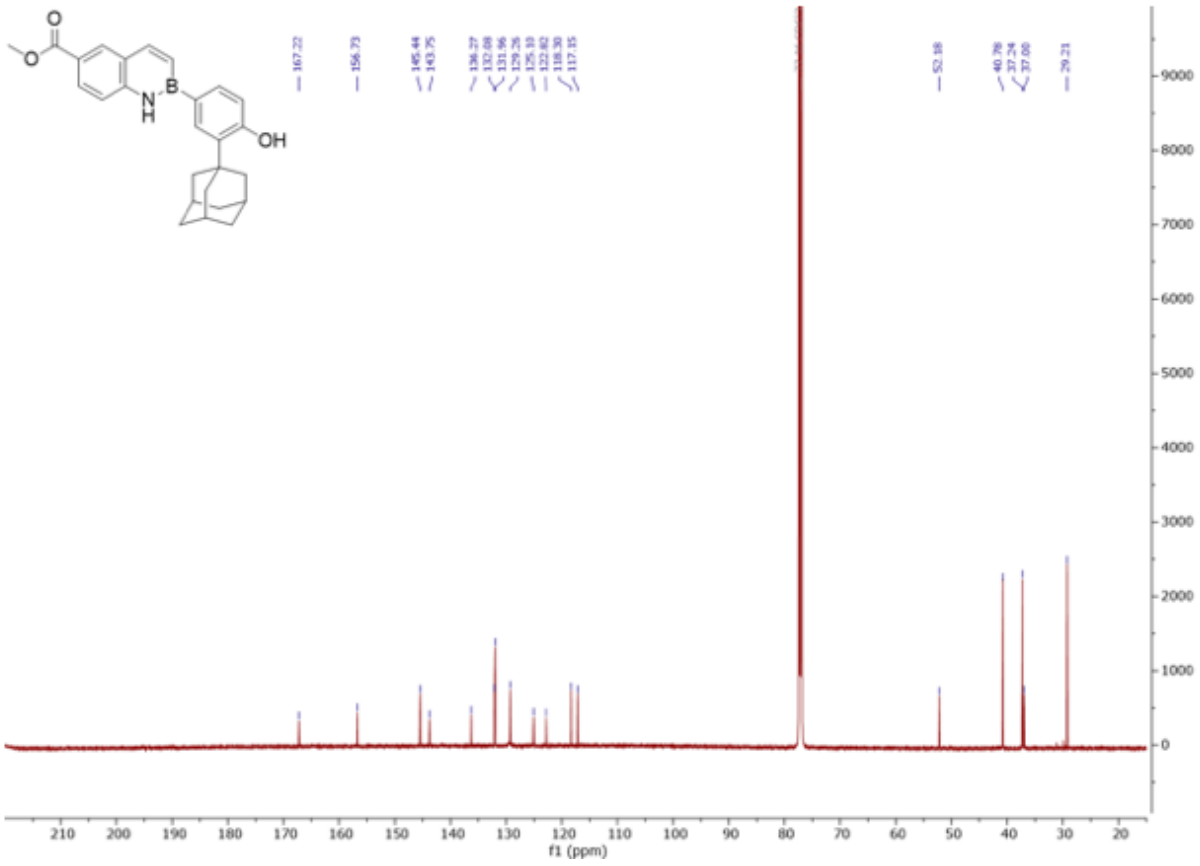
O
O
N
H
B
OH
167.22
156.73
145.44
143.75
136.27
132.69
131.96
129.26
125.33
122.82
118.30
117.15
52.18
40.78
37.24
37.00
29.21
9000
8000
7000
6000
5000
4000
3000
2000
1000
0
210
200
190
180
170
160
150
140
130
120
110
100
90
80
70
60
50
40
30
20
f1 (ppm)

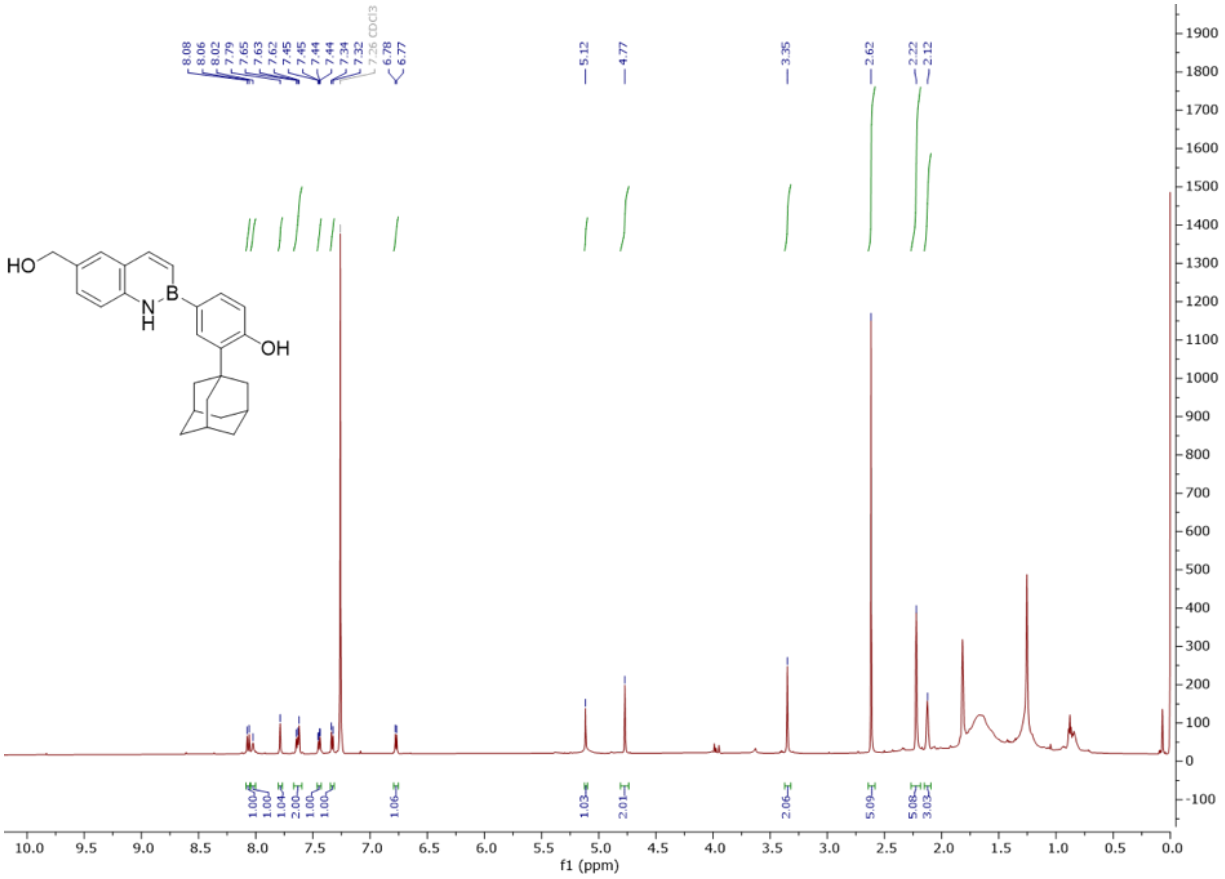
8.08
8.06
8.02
7.79
7.65
7.63
7.62
7.45
7.45
7.44
7.44
7.34
7.32
7.26 CDCl3
6.78
6.77
5.12
4.77
3.35
2.62
2.22
2.12
HO
N
H
B
OH
f1 (ppm)

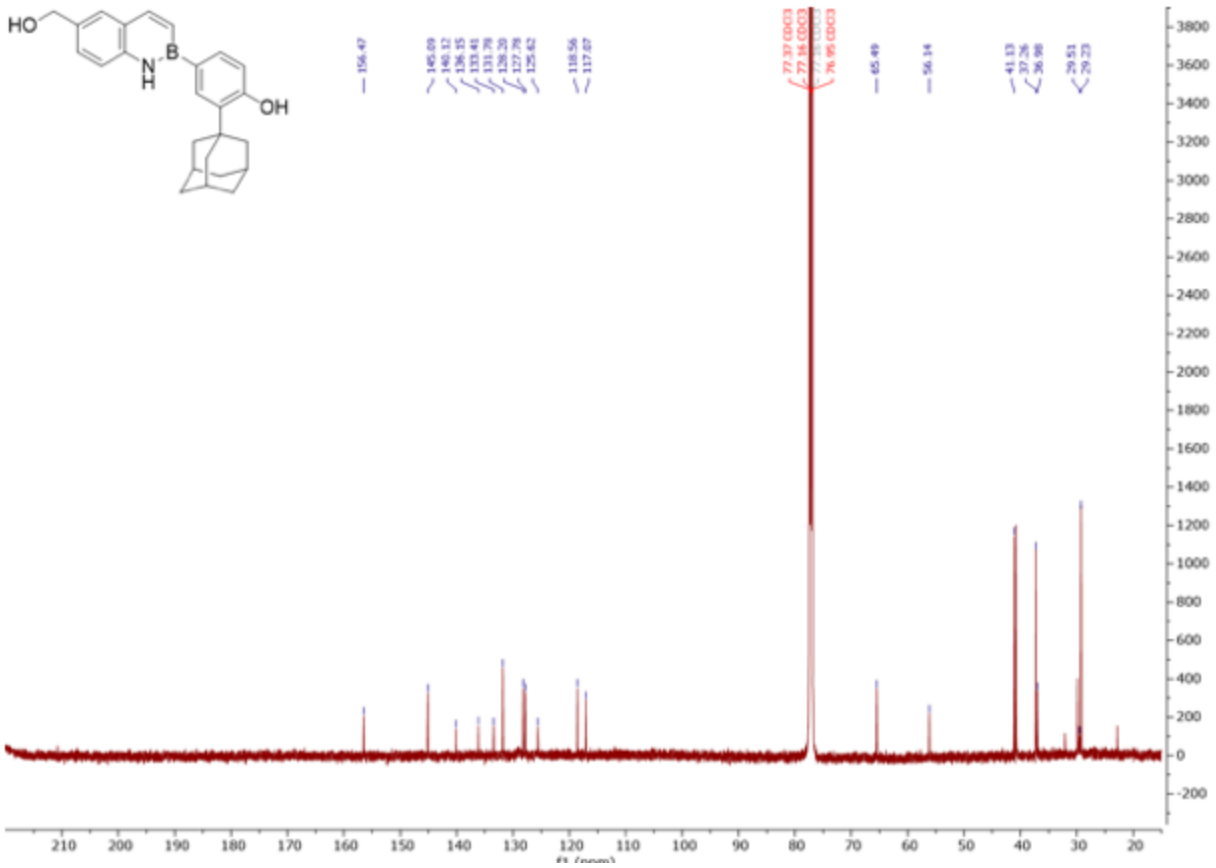
HO
N
H
B
OH
156.47
145.09
140.12
136.15
133.41
131.78
128.20
127.78
125.62
118.56
117.07
77.37 (DCl3)
77.16 (DCl3)
76.95 (DCl3)
65.49
56.14
41.13
37.26
36.98
29.51
29.23
f1 (ppm)

SF2768

Biology

For all minimum inhibitory concentration (MIC) assays, bacteria were grown in 5 mL of Mueller-Hinton broth (tryptic-soy broth for ATCC 33591) overnight with shaking at 37˚C. Lab strains of bacteria are as follows: methicillin susceptible *Staphylococcus aureus* (SH1000), hospital-acquired methicillin resistant *Staphylococcus aureus* (ATCC 33591), community-acquired methicillin resistant *Staphylococcus aureus* (USA 300-0114), *Pseudomonas aeruginosa* (PA01), *Enterococcus faecalis* (OG1RF), and *Escherichia coli* (MC4100).

Minimum Inhibitory Concentration assays

Each compound was serially diluted from 10% DMSO in sterile DI water (v/v) stock solutions with sterile DI water to yield 12 concentrations ranging from 500 µM to 0.250 µM. The overnight cultures for each bacterium were then inoculated into 5 mL of their respective fresh media and grown until exponential phase. Once in exponential phase, each bacteria was diluted to ca. 10^6 CFU/mL in Mueller-Hinton broth and 100 µL was added to each well of 96 well U-bottom plates (VWR 15705-064) containing 100 µL of each concentration to yield test concentrations ranging from 250µM to 0.125 µM. The bacteria were grown for 22-23 hours at 37˚C before visual inspection for the MIC, which was determined as the lowest concentration at which no growth could be seen to the naked eye over three independent trials. 10% DMSO in sterile DI water served as the positive control to confirm the concentration of DMSO was not responsible for cell death. Mueller-Hinton Broth served as the negative control, showing that the media was not contaminated.

Chemistry

[20] (R)-3-formamidobutanoic acid. Procedure followed exactly from:

Xu, Y; Tan, D.S., Total Synthesis of the Bacterial Diisonitrile Chalkophore SF2768, *Org. Lett.*, 2019, **21**, 8731-8735

^{1}H NMR 1H NMR (400 MHz, CDCl3) δ 8.11 – 8.09 (m, 1H), 4.51 – 4.38 (m, 1H), 3.48 (s, 3H), 2.65 – 2.46 (m, 3H), 1.31 (dd, J = 19.6, 6.8 Hz, 4H).

[21] 2,5-dioxopyrrolidin-1-yl (R)-3-formamidobutanoate. Procedure followed exactly from:

Xu, Y; Tan, D.S., Total Synthesis of the Bacterial Diisonitrile Chalkophore SF2768, *Org. Lett.*, 2019, **21**, 8731-8735

^{1}H NMR (600 MHz, CDCl3) δ 8.16 (s, 1H), 4.61 (p, J = 6.8 Hz, 1H), 4.18 – 4.10 (m, 1H), 3.00 – 2.95 (m, 1H), 2.88 (s, 3H), 2.85 – 2.80 (m, 1H), 1.38 (dd, J = 6.9, 1.3 Hz, 2H).

[22] 2,5-dioxopyrrolidin-1-yl (R)-3-isocyanobutanoate. Procedure followed exactly from:

Xu, Y; Tan, D.S., Total Synthesis of the Bacterial Diisonitrile Chalkophore SF2768, *Org. Lett.*, 2019, **21**, 8731-8735

^{1}H NMR (400 MHz, CDCl3) δ 4.16 (h, J = 6.8 Hz, 1H), 3.10 (dd, J = 16.4, 6.5 Hz, 1H), 2.95 – 2.78 (m, 5H), 1.55 (dt, J = 6.7, 1.9 Hz, 3H).

[24] di-tert-butyl (6-hydroxyhexane-1,5-diyl)(S)-dicarbamate. Procedure followed exactly from:

Xu, Y; Tan, D.S., Total Synthesis of the Bacterial Diisonitrile Chalkophore SF2768, *Org. Lett.*, 2019, **21**, 8731-8735

^{1}H NMR (600 MHz, CDCl3) δ 4.77 (s, 1H), 4.57 (s, 1H), 3.68 – 3.51 (m, 4H), 3.17 (dt, J = 13.6, 7.0 Hz, 1H), 3.09 (dd, J = 13.2, 6.6 Hz, 1H), 1.56 (d, J = 18.3 Hz, 2H), 1.53 – 1.47 (m, 3H), 1.44 (d, J = 3.4 Hz, 21H).

[25] (S)-2,6-bis((tert-butoxycarbonyl)amino)hexyl acetate. Procedure followed exactly from:

Xu, Y; Tan, D.S., Total Synthesis of the Bacterial Diisonitrile Chalkophore SF2768, *Org. Lett.*, 2019, **21**, 8731-8735

^{1}H NMR (600 MHz, CDCl3) δ 4.55 (s, 2H), 4.05 (qd, J = 11.2, 4.7 Hz, 2H), 3.83 (s, 1H), 3.11 (q, J = 6.7 Hz, 2H), 2.07 (s, 3H), 1.56 (s, 3H), 1.44 (d, J = 2.8 Hz, 20H).

[26] (S)-1-acetoxy-6-aminohexan-2-aminium 2,2,2-trifluoroacetate salt. Procedure followed exactly from:

Xu, Y; Tan, D.S., Total Synthesis of the Bacterial Diisonitrile Chalkophore SF2768, *Org. Lett.*, 2019, **21**, 8731-8735

^{1}H NMR (600 MHz, DMSO) δ 8.06 (s, 3H), 7.76 (s, 3H), 4.20 (dd, J = 12.0, 3.5 Hz, 1H), 4.05 (dd, J = 12.0, 6.7 Hz, 1H), 3.41 – 3.30 (m, 1H), 2.76 (tt, J = 11.5, 5.9 Hz, 2H), 2.06 (s, 3H), 1.61 – 1.49 (m, 4H), 1.38 (p, J = 7.9 Hz, 2H).

[14] (S)-2,6-bis((R)-3-isocyanobutanamido)hexyl acetate. Procedure followed exactly from:

Xu, Y; Tan, D.S., Total Synthesis of the Bacterial Diisonitrile Chalkophore SF2768, *Org. Lett.*, 2019, **21**, 8731-8735

^{1}H NMR (400 MHz, CDCl3) δ 6.71 (dd, J = 7.9, 4.2 Hz, 1H), 6.47 (d, J = 8.9 Hz, 1H), 4.18 (tdd, J = 10.8, 5.9, 2.0 Hz, 3H), 3.98 (h, J = 5.2 Hz, 2H), 3.69 – 3.59 (m, 1H), 2.82 – 2.70 (m, 1H), 2.48 (td, J = 13.3, 10.4 Hz, 2H), 2.37 – 2.25 (m, 2H), 2.00 (s, 3H), 1.69 – 1.46 (m, 4H), 1.47 – 1.37 (m, 7H), 1.39 – 1.30 (m, 2H).

[15] (3R,3'R)-N,N'-((S)-6-hydroxyhexane-1,5-diyl)bis(3-isocyanobutanamide). Procedure followed exactly from:

Xu, Y; Tan, D.S., Total Synthesis of the Bacterial Diisonitrile Chalkophore SF2768, *Org. Lett.*, 2019, **21**, 8731-8735

^{1}H NMR (600 MHz, DMSO) δ 7.97 (t, J = 5.7 Hz, 1H), 7.74 (d, J = 8.5 Hz, 1H), 4.63 (t, J = 5.5 Hz, 1H), 4.07 (q, J = 7.0 Hz, 2H), 3.70 (d, J = 4.9 Hz, 1H), 3.30 – 3.21 (m, 2H), 3.04 (tt, J = 14.5, 6.6 Hz, 2H), 2.50 – 2.42 (m, 4H), 2.38 (ddd, J = 14.0, 7.0, 3.8 Hz, 2H), 1.54 (d, J = 13.6 Hz, 1H), 1.45 – 1.21 (m, 11H).

[16] (R)-N-benzyl-3-isocyanobutanamide. To a flame dried round bottom flask equipped with a stir bar, phenylmethanamine (1.0 eq, 23mg, 0.22 mmol) was dissolved in trifluoroacetic acid (0.2M, 1.1mL) and N,N-Diisopropylethylamine (1.5 eq, 0.06mL). This mixture was then cooled to 0°C. [**22**] (1.0 eq, 50 mg, 0.24 mmol) was then added in portions. The mixture was then warmed to room temperature and stirred for six hours. Once complete by TLC, the reaction mixture was quenched with water (4 mL). The organic layer was extracted (3x, 10 mL) and washed with brine (10 mL). The combined organic layers were then dried with magnesium sulfate, concentrated, and purified by flash chromatography in 100% ethyl acetate to afford the product (25 mg, 57% yield).

^{1}H NMR (600 MHz, DMSO) δ 8.38 (t, J = 6.0 Hz, 1H), 7.95 (dd, J = 32.9, 5.1 Hz, 2H), 7.36 – 7.19 (m, 5H), 4.26 (d, J = 6.0 Hz, 2H), 4.18 (ddd, J = 14.2, 7.6, 5.9 Hz, 1H), 2.41 – 2.19 (m, 2H), 1.09 (dd, J = 30.2, 6.7 Hz, 3H).

^{13}C NMR (151 MHz, DMSO) δ 170.23, 163.99, 160.60, 139.99, 128.72, 127.68, 127.20, 45.49, 43.93, 42.47, 42.34, 41.51, 40.42, 40.28, 40.14, 40.00, 39.86, 39.72, 39.58, 20.57.

Spectra

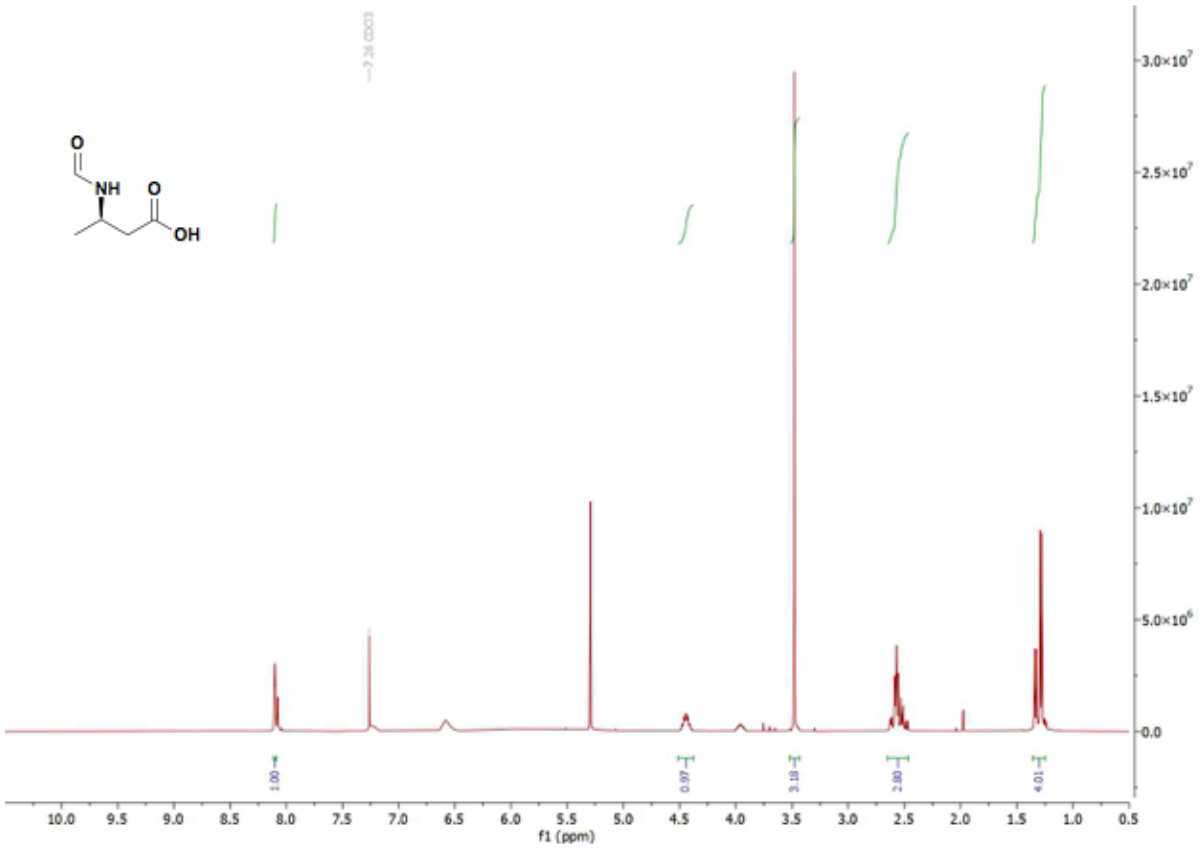
O
NH
O
OH
3.0×10^7
2.5×10^7
2.0×10^7
1.5×10^7
1.0×10^7
5.0×10^6
0.0
1.00
0.97
3.18
2.80
4.01
10.0
9.5
9.0
8.5
8.0
7.5
7.0
6.5
6.0
5.5
5.0
4.5
4.0
3.5
3.0
2.5
2.0
1.5
1.0
0.5
f1 (ppm)

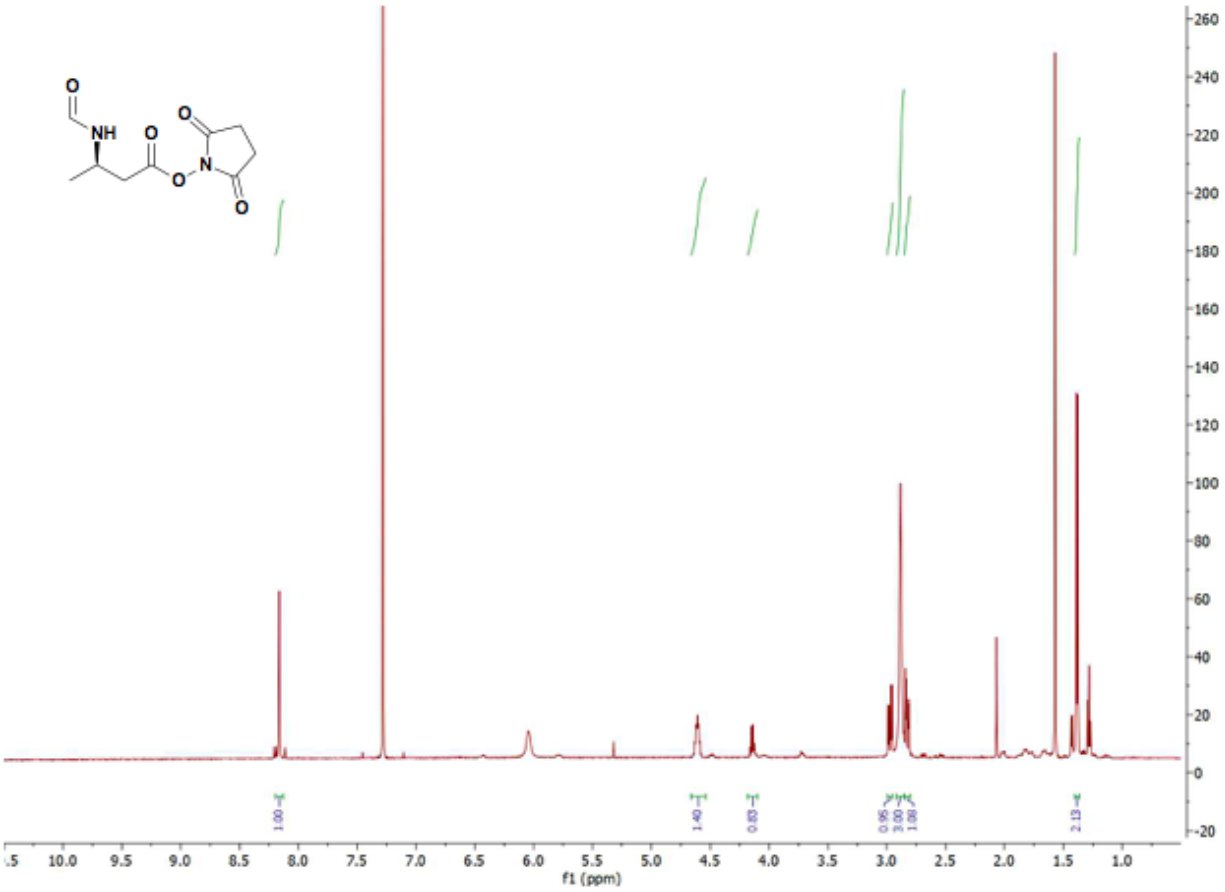
O
NH
O
O
O
N
O
260
240
220
200
180
160
140
120
100
80
60
40
20
0
-20
1.00
1.49
0.83
0.95
3.00
1.08
2.13
10.0
9.5
9.0
8.5
8.0
7.5
7.0
6.5
6.0
5.5
5.0
4.5
4.0
3.5
3.0
2.5
2.0
1.5
1.0
f1 (ppm)

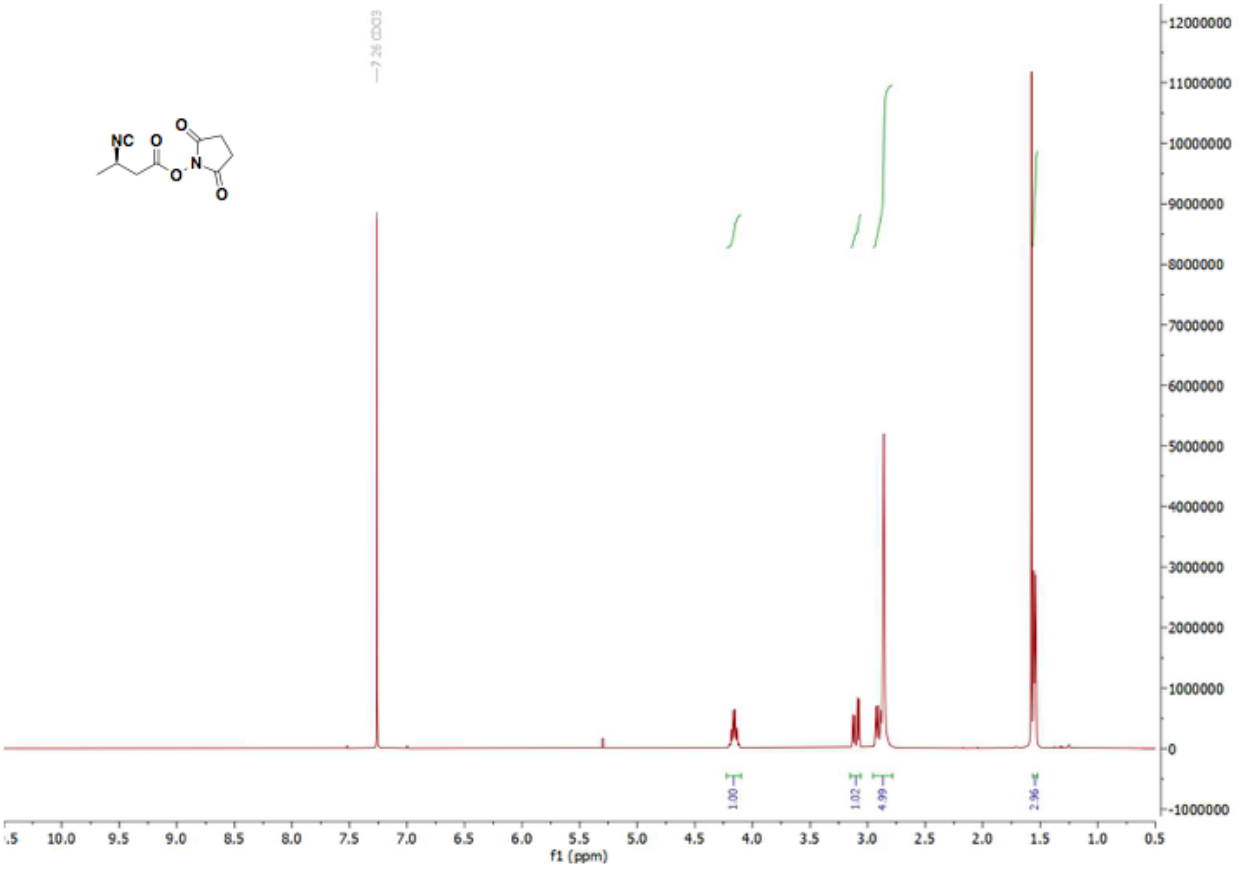
NC
O
O
O
N
O
7.26 CDCl3
12000000
11000000
10000000
9000000
8000000
7000000
6000000
5000000
4000000
3000000
2000000
1000000
0
-1000000
1.00
1.02
4.99
2.96
10.0
9.5
9.0
8.5
8.0
7.5
7.0
6.5
6.0
5.5
5.0
4.5
4.0
3.5
3.0
2.5
2.0
1.5
1.0
0.5
f1 (ppm)

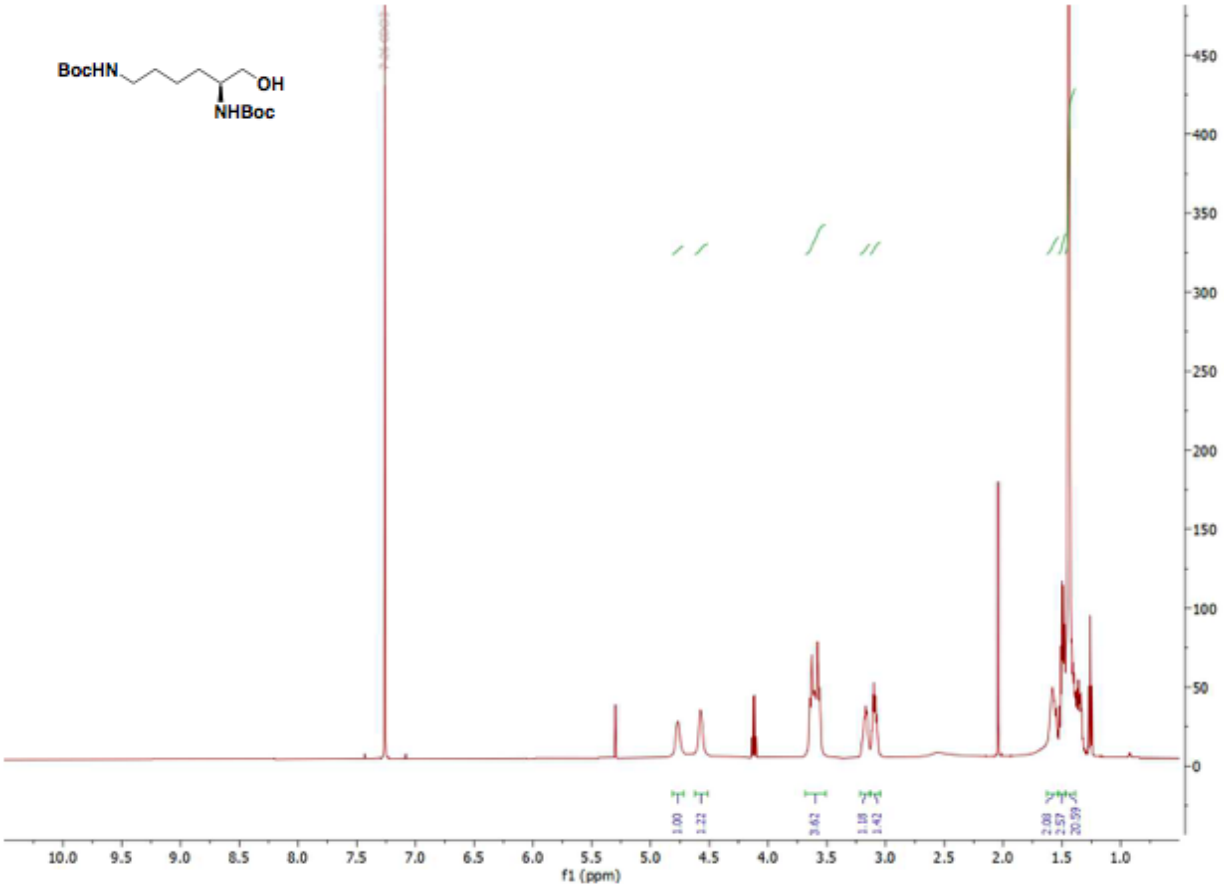
BocHN
OH
NHBoc
450
400
350
300
250
200
150
100
50
0
1.00
1.22
3.62
1.18
3.42
2.08
2.57
20.59
10.0
9.5
9.0
8.5
8.0
7.5
7.0
6.5
6.0
5.5
5.0
4.5
4.0
3.5
3.0
2.5
2.0
1.5
1.0
f1 (ppm)

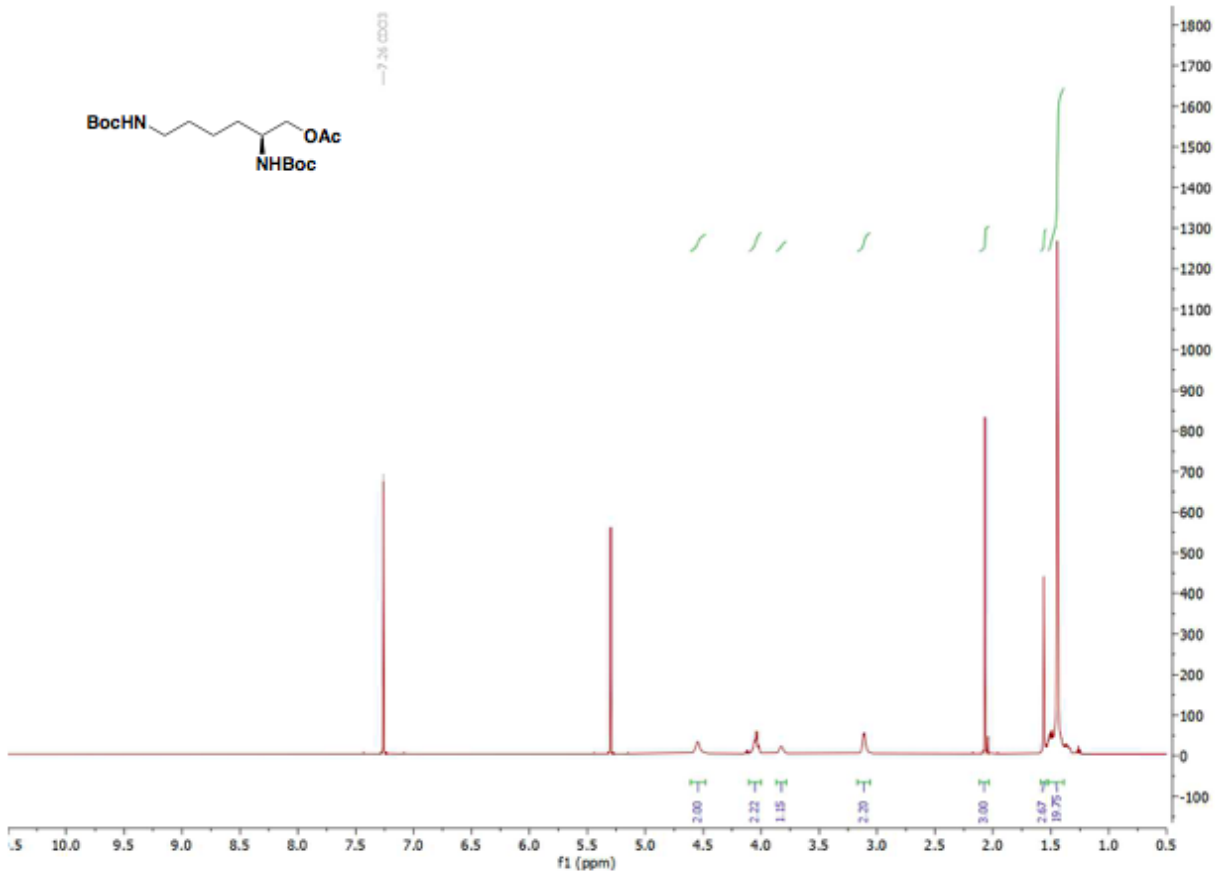
BocHN
OAc
NHBoc
f1 (ppm)

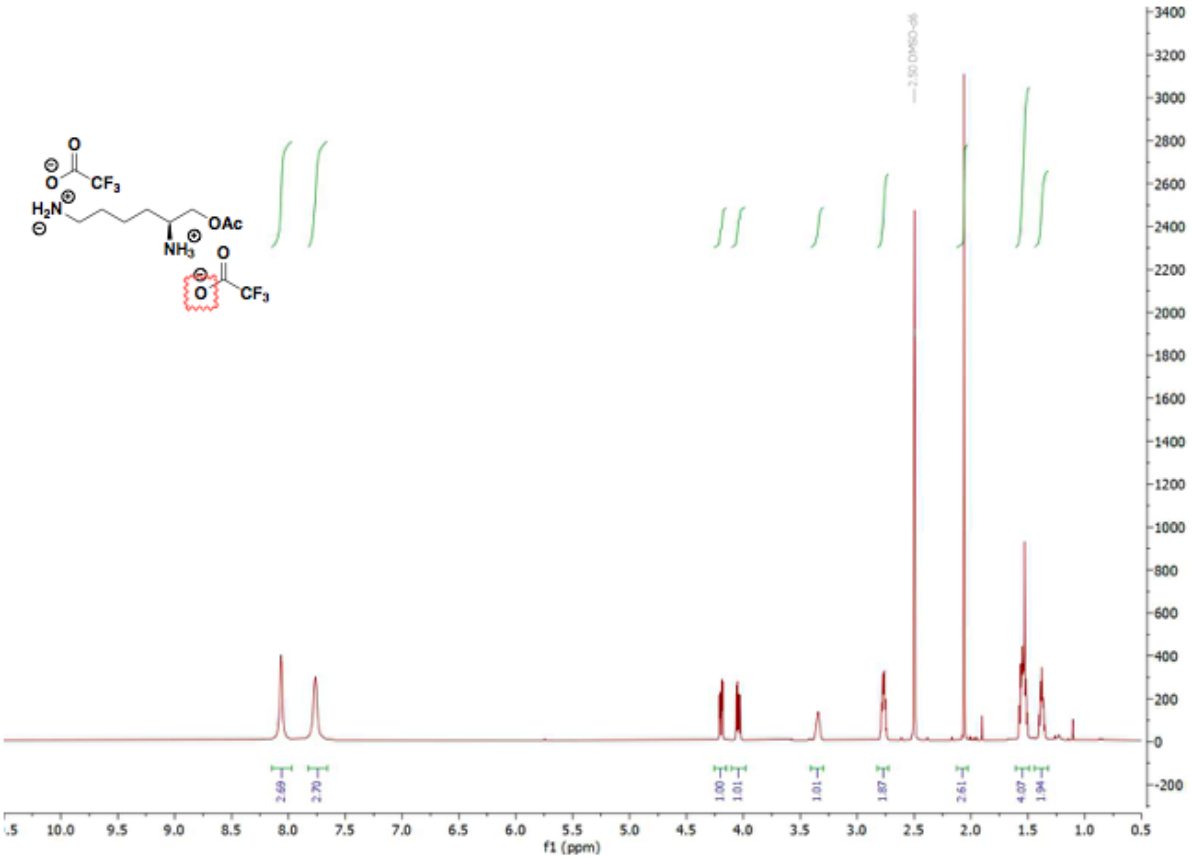
f1 (ppm)

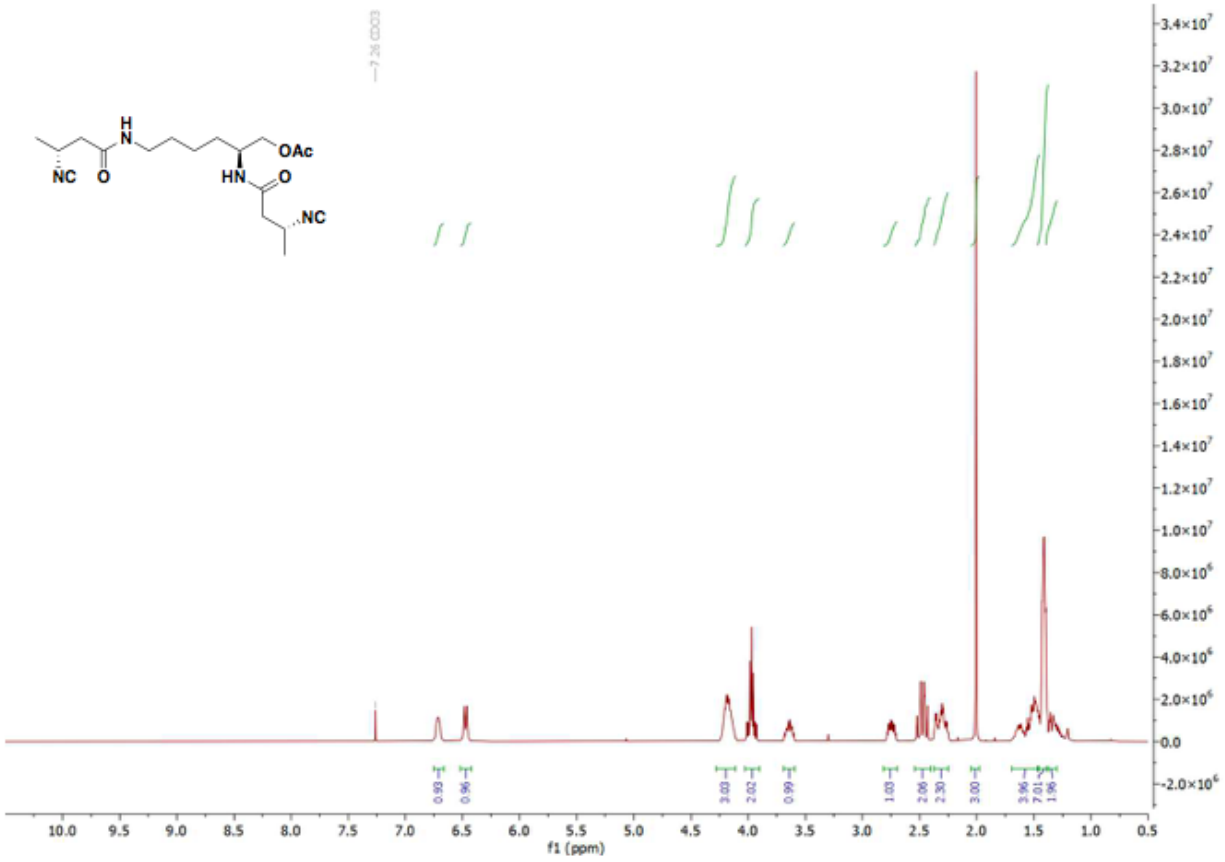
NC
O
H
N
HN
O
OAc
NC
f1 (ppm)

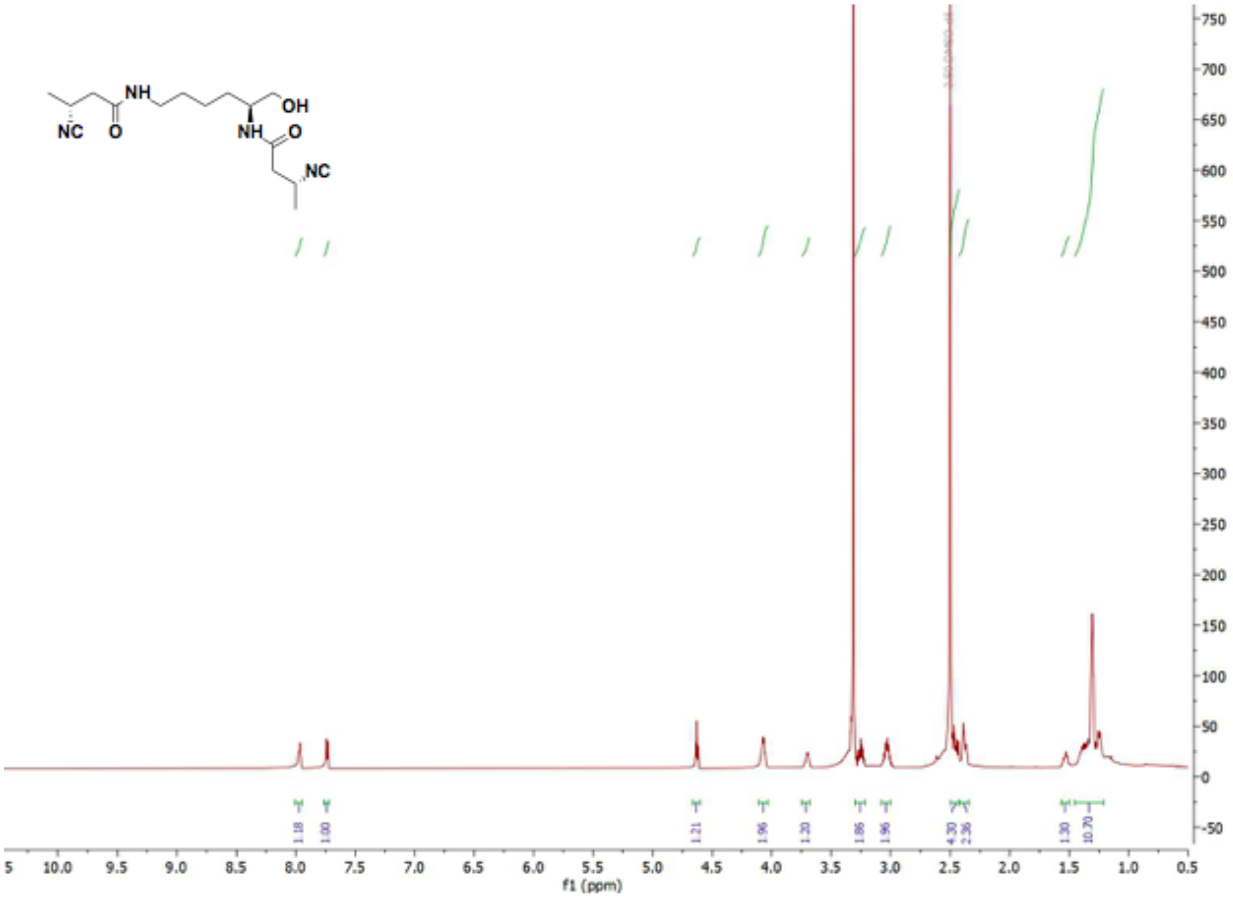
NC
O
NH
OH
NH
O
NC
f1 (ppm)

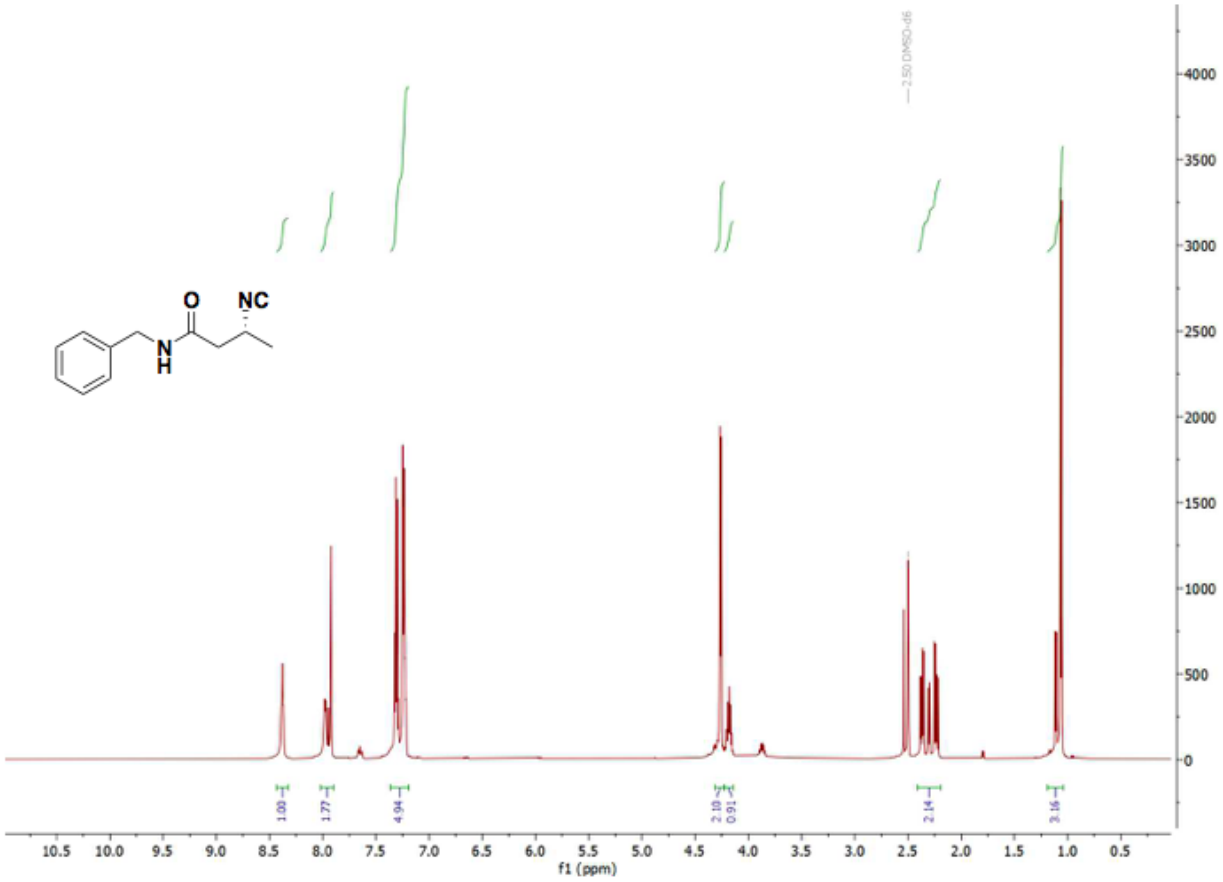
O
NC
N
H
2.50 DMSO-d6
4000
3500
3000
2500
2000
1500
1000
500
0
1.00
1.77
4.94
2.10
0.91
2.14
3.16
10.5
10.0
9.5
9.0
8.5
8.0
7.5
7.0
6.5
6.0
5.5
5.0
4.5
4.0
3.5
3.0
2.5
2.0
1.5
1.0
0.5
f1 (ppm)

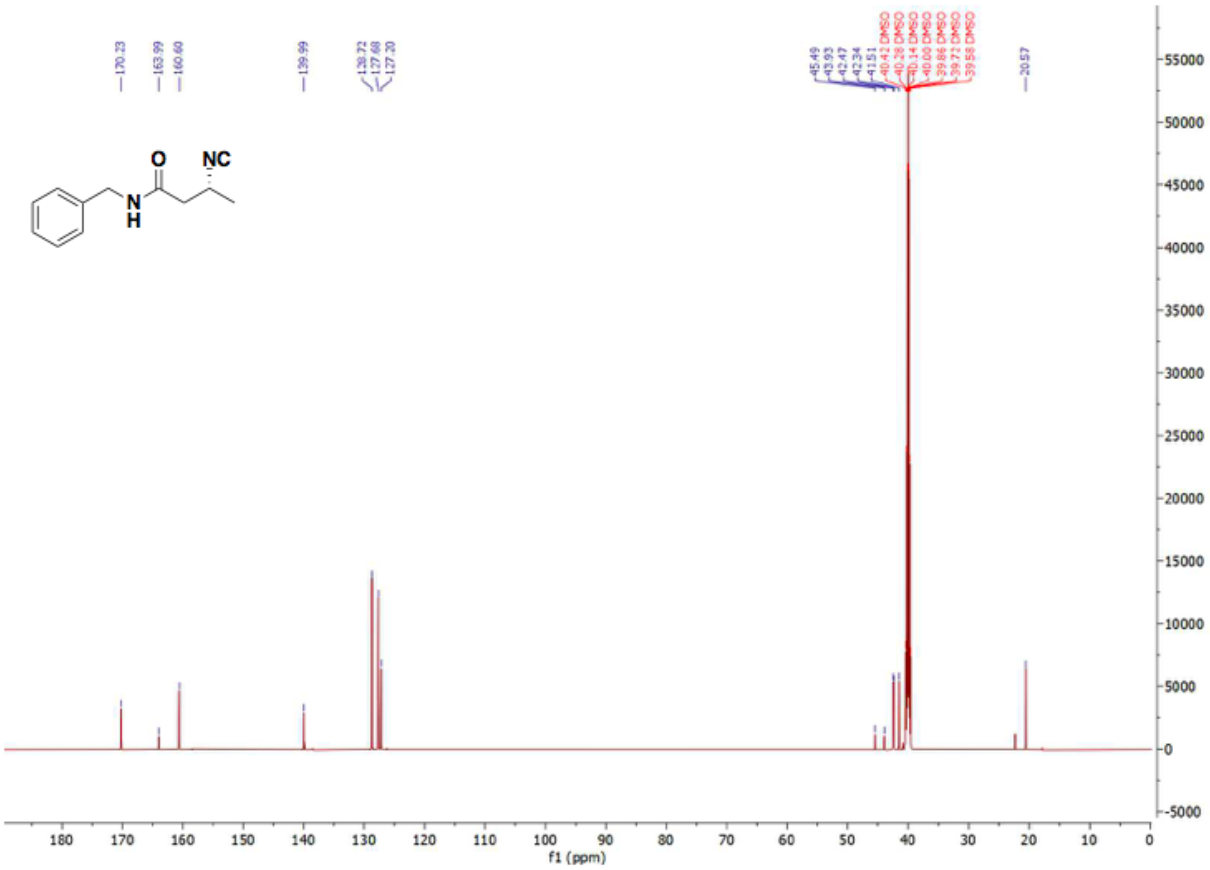
170.23
163.99
160.60
139.99
130.72
127.68
127.20
45.49
43.93
42.47
42.34
41.51
40.42 DMSO
40.28 DMSO
40.14 DMSO
40.00 DMSO
39.86 DMSO
39.72 DMSO
39.58 DMSO
20.57
O
NC
N
H
55000
50000
45000
40000
35000
30000
25000
20000
15000
10000
5000
0
-5000
180
170
160
150
140
130
120
110
100
90
80
70
60
50
40
30
20
10
0
f1 (ppm)

References:

[1] Durão, P.; Balbontín, R.; Gordo, I., Evolutionary Mechanisms Shaping the Maintenance of Antibiotic Resistance, *Trends Microbiol.*, 2018, **26**, 677-691

[2] Biggest Threats and Data, Centers for Disease Control and Prevention, 18 Sept 2020. www.cdc.gov/drugresistance/biggest-threats.html.

[3] Van Hoek A. H. A. M.; Mevius, D.; Guerra, B.; Mullany, P.; et al., Acquired antibiotic resistance genes: an overview, *Front. Microbiol.*, 2011, **2**

[4] Lewis, K. Persister Cells. *Annu. Rev. Microbiol.* 2010, **64**, 357-372

[5] Schrank, C.L.; Wilt, I.K.; Ortiz, C.M.; Haney, B.A.; Wuest, W. M. Using membrane perturbing small molecules to target chronic persistent infections, *RCS Med. Chem.* 2021, **12**, 1312-1324

[6] Kim, W.; Zou, G.; Hari, T. P. A.; Eleftherios Mylonakis, E.; et al. A selective membrane-targeting repurposed antibiotic with activity against persistent methicillin-resistant Staphylococcus aureus, *Proc. Natl. Acad. Sci.*, 2019, **116**, 33

[7] Kenney, G. E.; Rosenzweig, A.C., Chalkophores, Annu. Rev. Biochem., 2018., **87**, 645-676

[8] Xu, Y.; Tan, D.S. Total Synthesis of the Bacterial Diisonitrile Chalkophore SF2768, *Org. Lett.*, 2019, **21**, 8731−8735

[9] Johnson, CL.; Mendonca, A.F.; DiSpirito, A.A.; Pometto, A.L.; Dickenson, J.S. Methanobactin: a potential novel biopreservative for use against the foodborne pathogen
Listeria monocytogenes, Ph.D. Thesis, Iowa State Univ., 2006

[10] Kim, W.; Zhu, W.; Hendricks, G.L.; Tyne, D.; et al. A new class of synthetic retinoid antibiotics effective against bacterial persisters, *Nature*, 2018, **556**, 103-107

[11] A.V. Cheng, A.V.; Kim, W.; Escobar, I.E.; Mylonakis, E.; Wuest, W.M. Structure-activity relationship and anticancer profile of second-generation anti-MRSA synthetic retinoids, *ACS Med. Chem. Lett.,* 2020, **11**, 393-397

[12] Cheng, A.V.; Schrank C.L.; Escobar, I.E.; Mylonakis, E.; Wuest W.M., Addition of ethylamines to the phenols of bithionol and synthetic retinoids does not elicit activity in gram-negative bacteria, *Bioorg. Med. Chem. Lett.*, 2020, **30,** 127099

[13] Z. Liu, Z.; T.B. Marder, T.B., B-N versus C-C: how similar are they?, *Angew. Chem. Int. Ed*., 2008, **47**, 242-244

[14] Bonifazi, D.; Fasano, F.; Lorenzo-Garcia, M.M.; Marinelli, D.; et al., Boron–nitrogen doped carbon scaffolding: organic chemistry, self-assembly and materials applications of borazine and its derivatives, *Chem. Comm.*, 2015, **51,** 83, 15222-15236

[15] Liu, L.; A.J.V. Marwitz, A.J.V.; Matthews, B.W.; S. Liu, Boron mimetics: 1,2-dihydro-1,2-azaborines bind inside a nonpolar cavity of T4 lysozyme, *Angew. Chem. Int. Ed. Engl.*, 2009, **48**, 37, 6817-6819

[16] Wisniewski, S.R.; Guenther, C.L.; Argintaru, O.A.; Molander, G.A., A convergent, modular approach to functionalized 2,1-borazaronaphthalenes from 2-aminostyrenes and potassium organotrifluoroborates, *J. Org. Chem.*, 2014, **79**, 365-378

[17] Haney, B.A.; Schrank, C.L.; Wuest, W.M., Synthesis and biological evaluation of an antibacterial azaborine retinoid isostere, *Tet. Let.*, 2021, **62**

[18]CLSI, M07-A9: Methods for Dilution Antimicrobial Susceptibility Tests for Bacteria That Grow Aerobically; Approved Standard-9th ed., 2012, pp. 1-88.

[19] OECD, Test No. 117: Partition Coefficient (n-octanol/water), HPLC Method, OECD Guidelines for the Testing of Chemicals, Section 1, OECD Publishing, Paris, 2004.

[20]Xu, Y; Tan, D.S., Total Synthesis of the Bacterial Diisonitrile Chalkophore SF2768, *Org. Lett.*, 2019, **21**, 8731-8735

[21] Amano, S.; Sakurai, T.; Endo, K.; Takano, H.; Beppu, T.; Furihata, K.; Sakuda, S.; Ueda, K., A cryptic antibiotic triggered by monensin, *J. Antibiot. Res.*, 2011, **64**, 703

[22] Wang, L.; Zhu, M.; Zhang, Q.; Zhang, X.; et al., Diisonitrile Natural Product SF2768 Functions As a Chalkophore That Mediates Copper Acquisition in Streptomyces thioluteus, *ACS Chem. Biol.* 2017, **12**, 3067-3075

[23] Hu̇bner, I.; Shapiro, J.A.; Hoßmann, J.; Drechsel, J.; Hacker, S.M.; Rather, P.N.;Pieper, D.H.; Wuest, W.M.; Sieber, S.A.; Broad Spectrum Antibiotic Xanthocillin X Effectively Kills Acinetobacter baumannii via Dysregulation of Heme Biosynthesis, *ACS Cent. Sci.*, 2021, **7**, 488-498